UHECR 2014 October 12-15, Springdale Utah

Radio detection of air showers with LOFAR and AERA

NIKHEF

IN·DEI·NOMINE·FELICITER

Jörg R. Hörandel Radboud University Nijmegen http://particle.astro.ru.nl

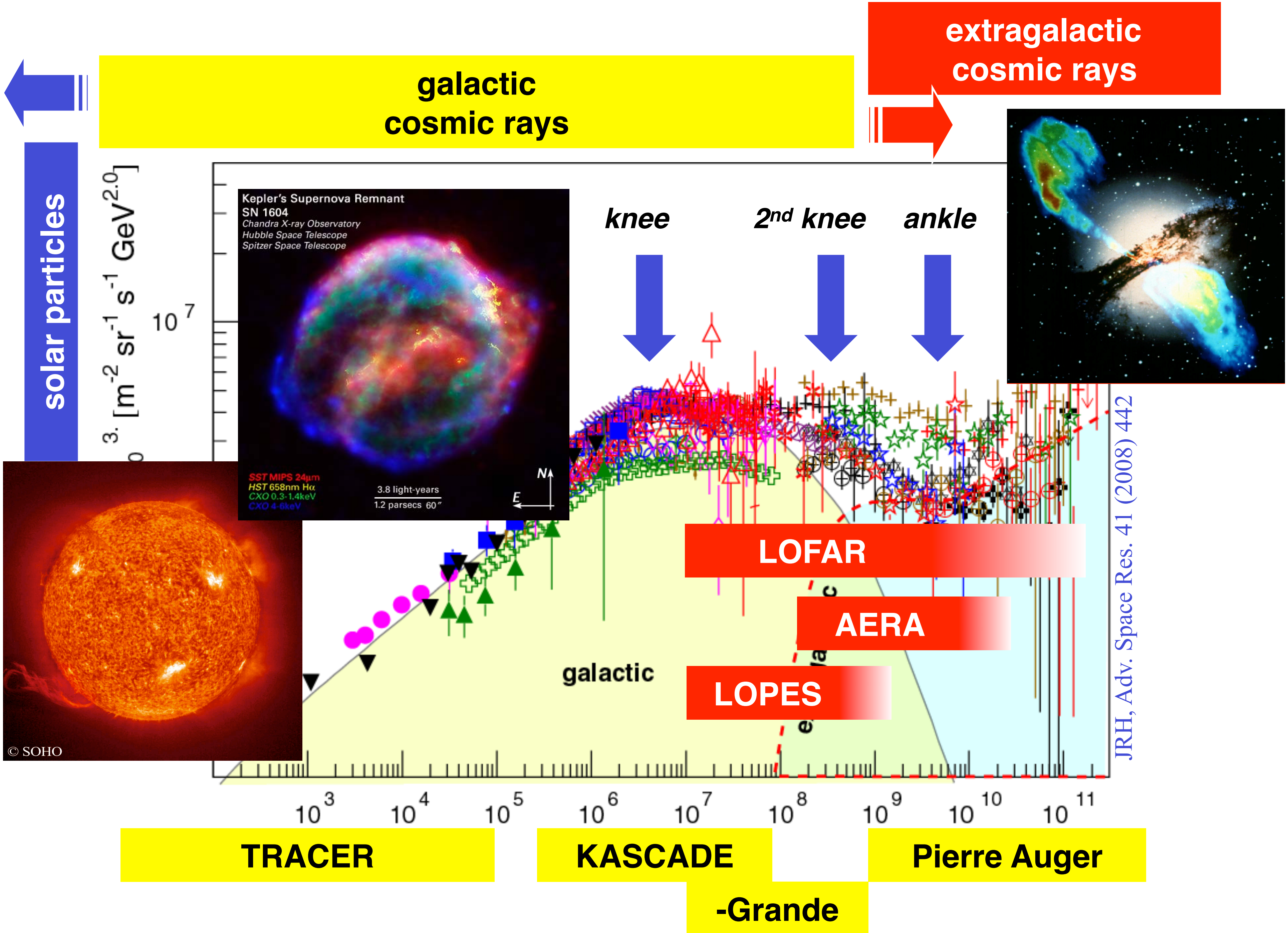

galactic
cosmic rays
extragalactic
cosmic rays
solar particles
[m^-2 sr^-1 s^-1 GeV^2.0]
10 7
Kepler's Supernova Remnant
SN 1604
Chandra X-ray Observatory
Hubble Space Telescope
Spitzer Space Telescope
SST MIPS 24μm
HST 658nm Hα
CXO 0.3-1.4keV
CXO 4-6keV
3.8 light-years
1.2 parsecs 60″
knee
2nd knee
ankle
LOFAR
AERA
LOPES
galactic
JRH, Adv. Space Res. 41 (2008) 442
© SOHO
10 3
10 4
10 5
10 6
10 7
10 8
10 9
10 10
10 11
TRACER
KASCADE
-Grande
Pierre Auger

Radio Emission in Air Showers

- Mainly: Charge separation in geomagnetic field

$$\vec{E} \propto \vec{v} \times \vec{B}$$

Theory predicts additional mechanisms:

- excess of electrons in shower: charge excess
- superposition of emission due to Cherenkov effects in atmosphere

polarization of radio signal

geomagnetic effect

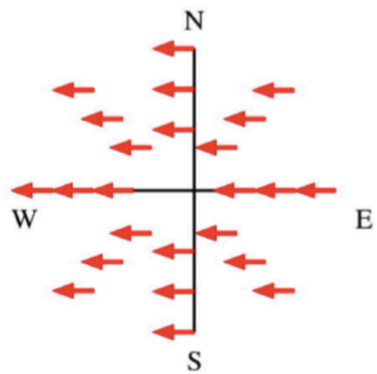

charge excess

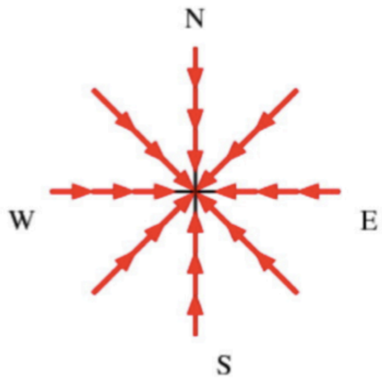

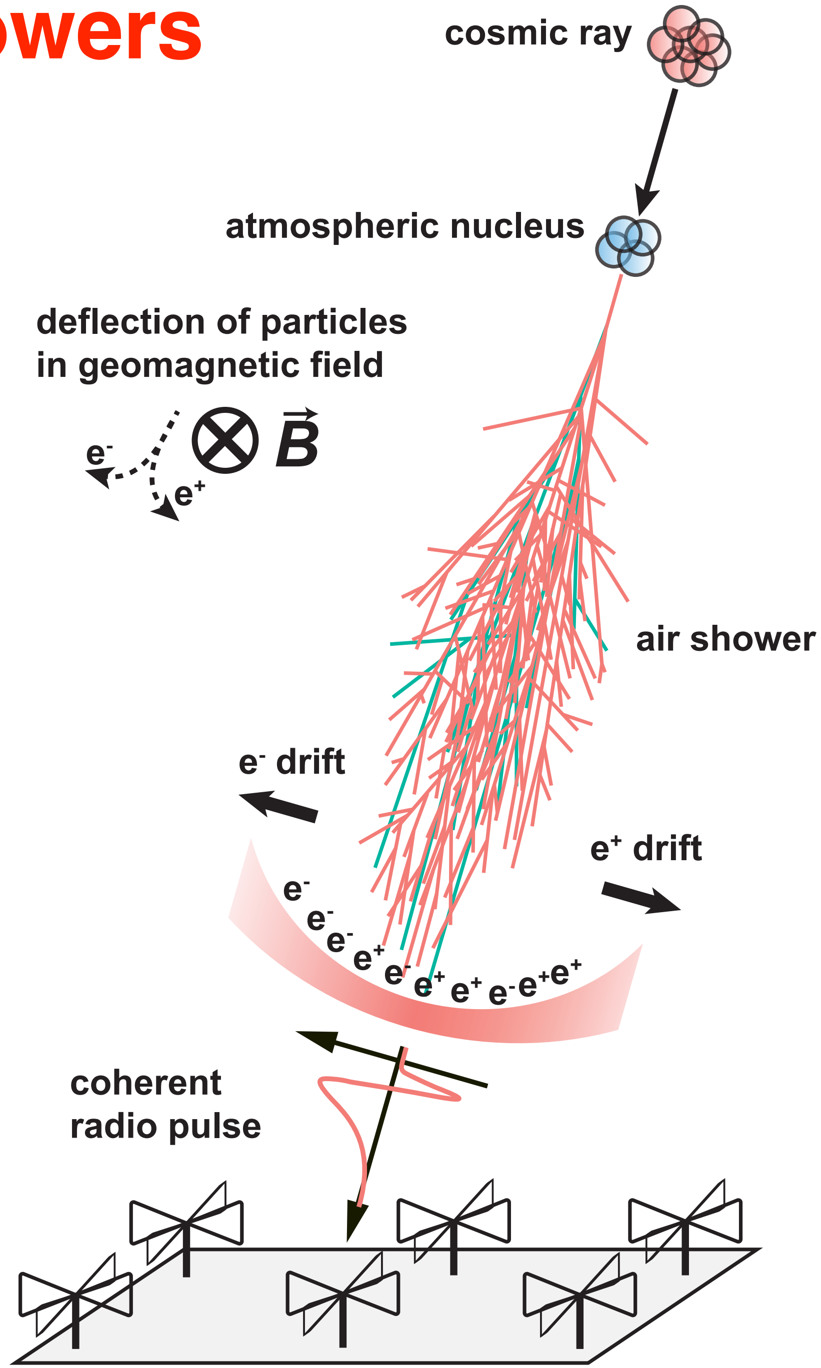

Radio Detectors

to measure properties of cosmic rays
- direction
- energy
- mass/type of particle

with ~100% duty cycle

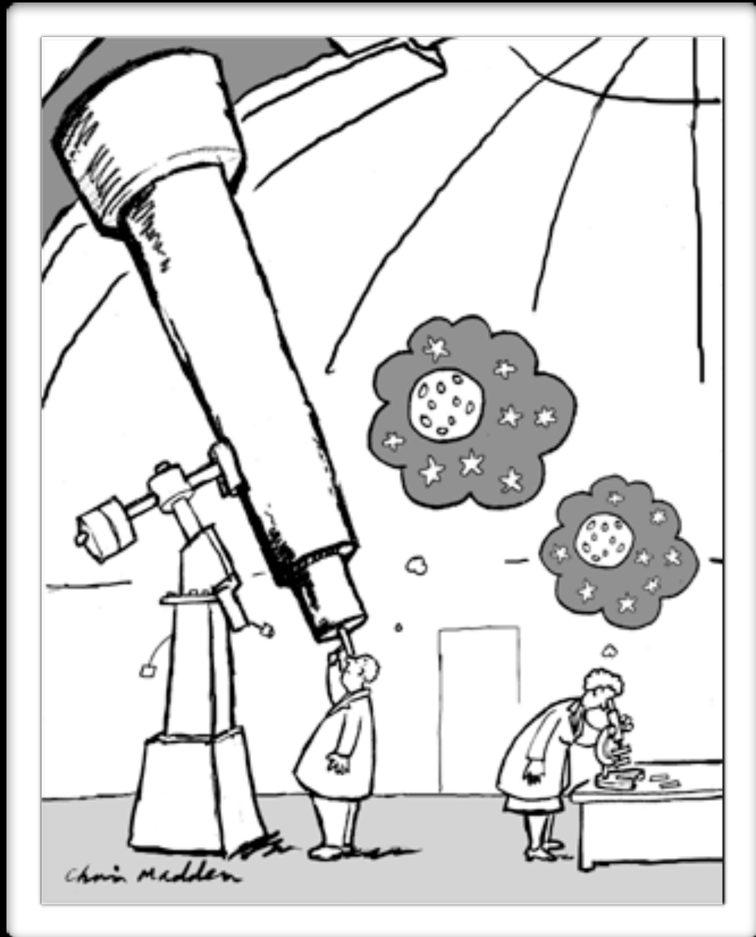

Large-scale radio detectors to measure extensive air showers

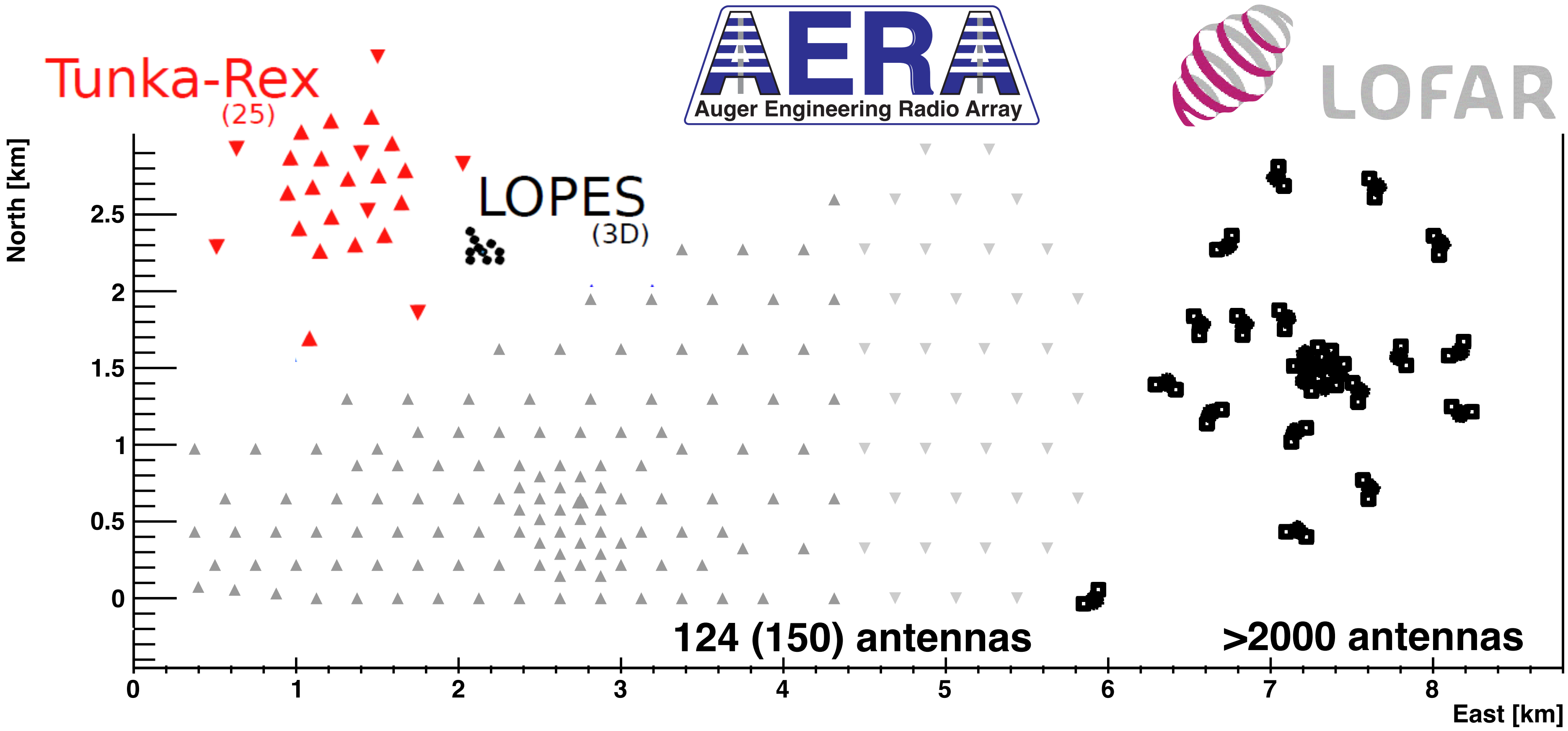

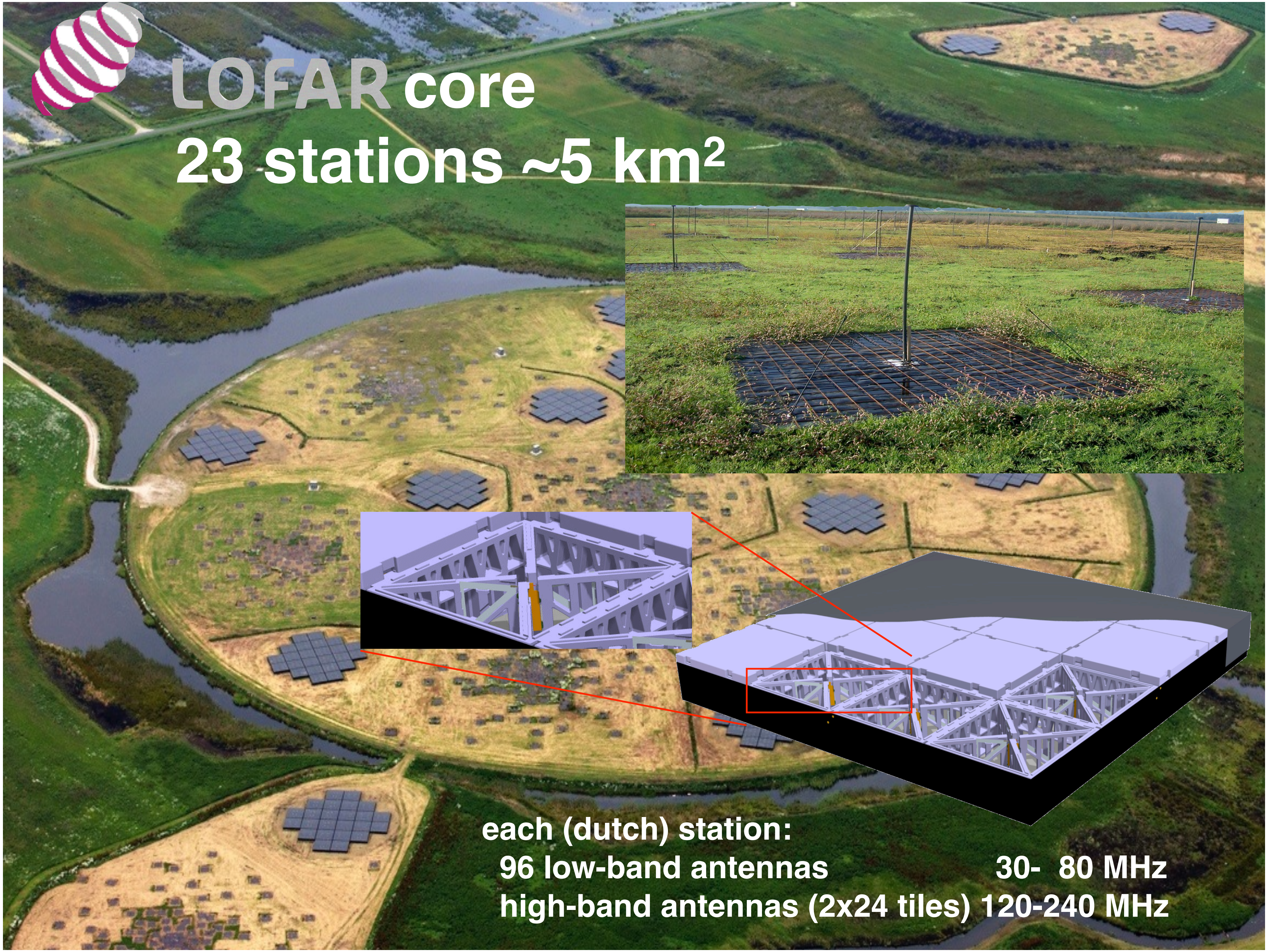
LOFAR core
23 stations ~5 km²
each (dutch) station:
96 low-band antennas 30- 80 MHz
high-band antennas (2x24 tiles) 120-240 MHz

LOFAR Radboud Air Shower Array - LORA

20 scintillator units
(~1 m² each)
read out by
wavelength shifter
bar and PMT
in LOFAR core

→ provide

- properties of EAS
- and trigger

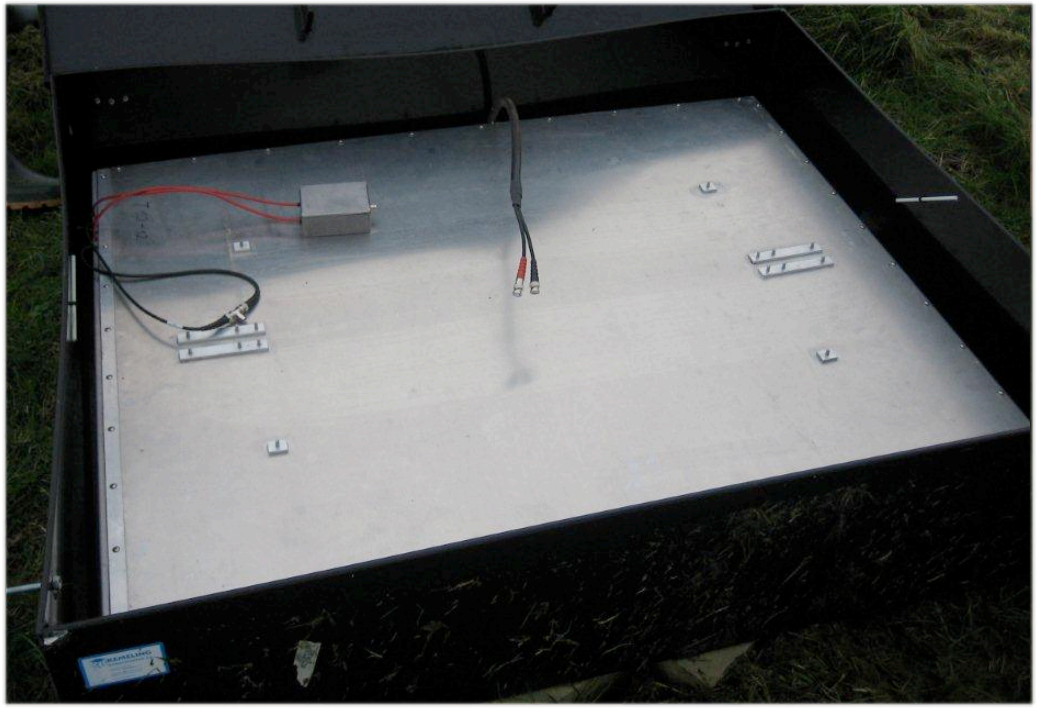

A measured air shower

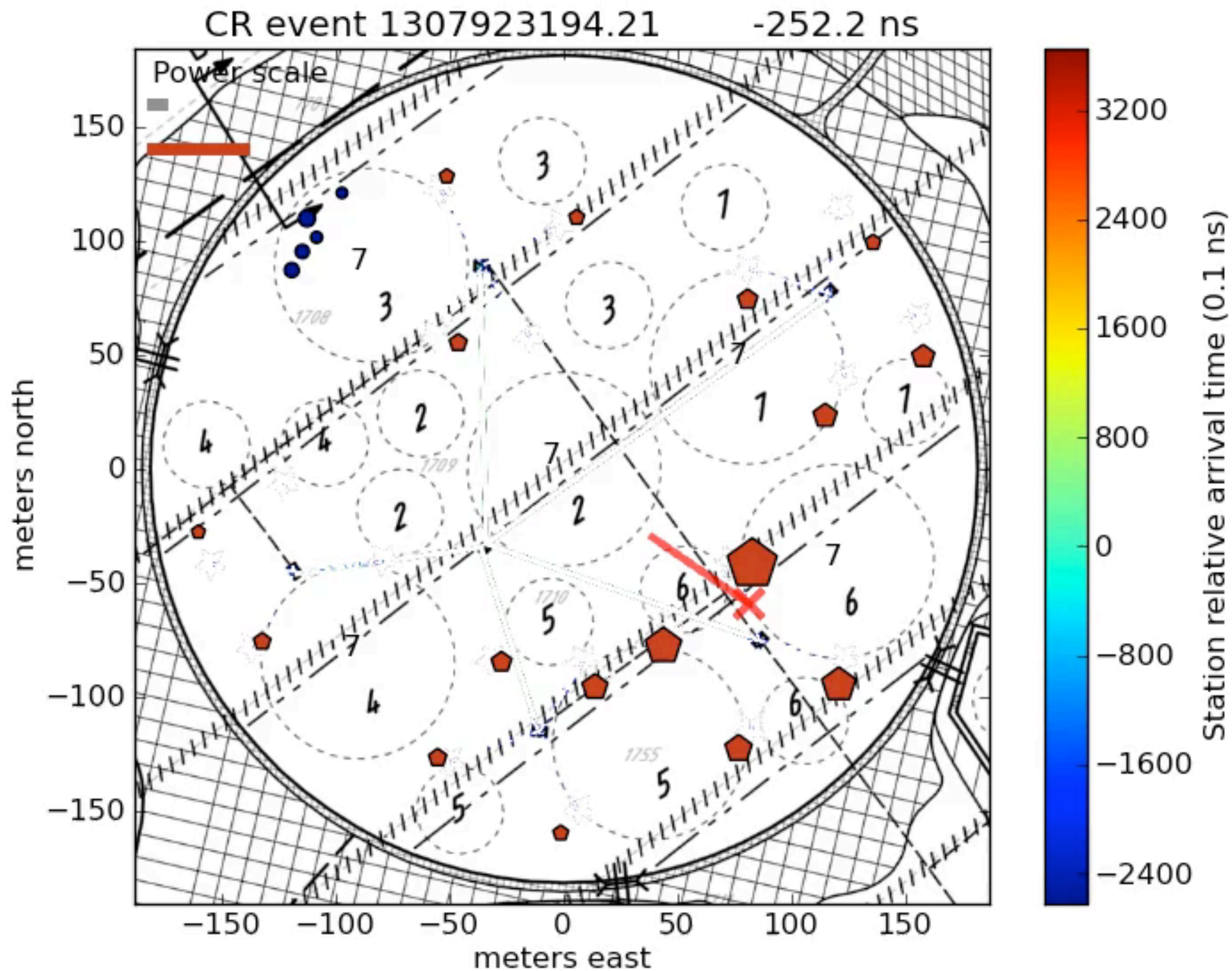

Circles: LOFAR antennas, Pentagons: LORA particle detectors, size denotes signal strength

The Auger Engineering Radio Array

PIERRE AUGER OBSERVATORY

AERA
Auger Engineering Radio Array

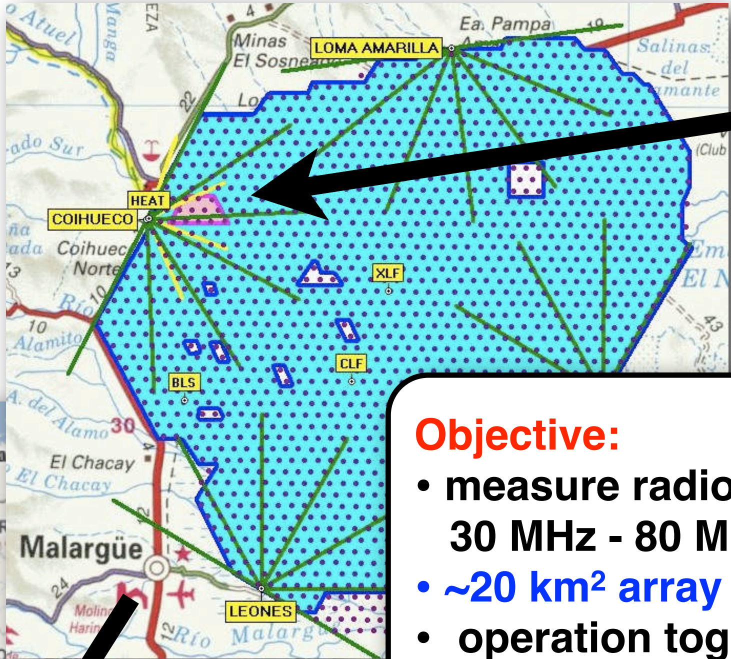

Objective:

- measure radio emission from EAS in frequency range 30 MHz - 80 MHz
- ~20 km² array with ~160 antennas
- operation together with infill/HEAT/AMIGA
- three antenna spacings to cover efficiently $17.2 < \lg E/\mathrm{eV} < 19.0$
- measure composition of cosmic rays in energy region of transition from galactic to extragalactic cosmic rays

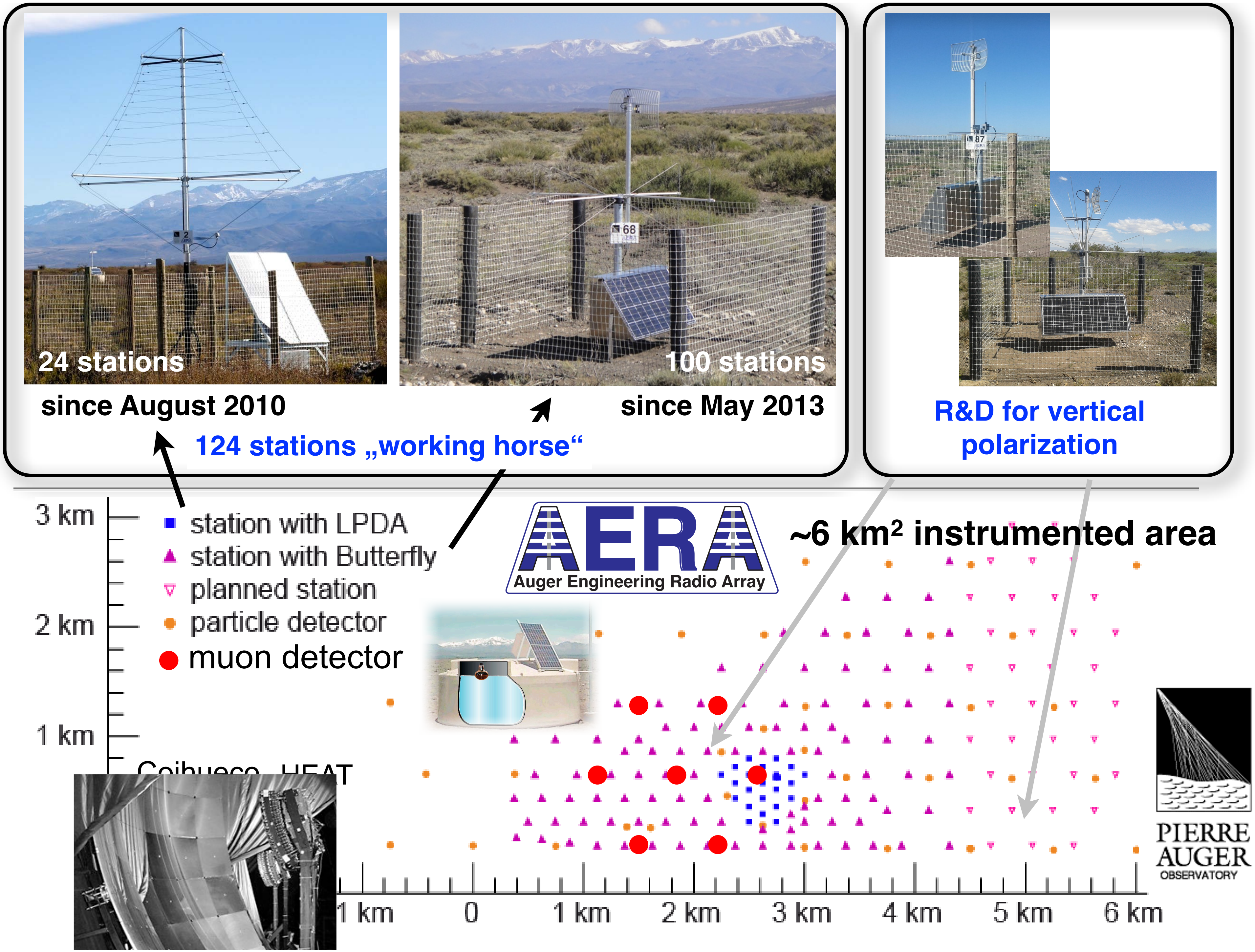

24 stations
100 stations
since August 2010
since May 2013
124 stations „working horse“
R&D for vertical polarization
station with LPDA
station with Butterfly
planned station
particle detector
muon detector
AERA
Auger Engineering Radio Array
~6 km² instrumented area
3 km
2 km
1 km
Coihueco HEAT
-1 km
0
1 km
2 km
3 km
4 km
5 km
6 km
PIERRE AUGER OBSERVATORY

An air shower measured simultaneously with ...

the Fluorescence Telescopes

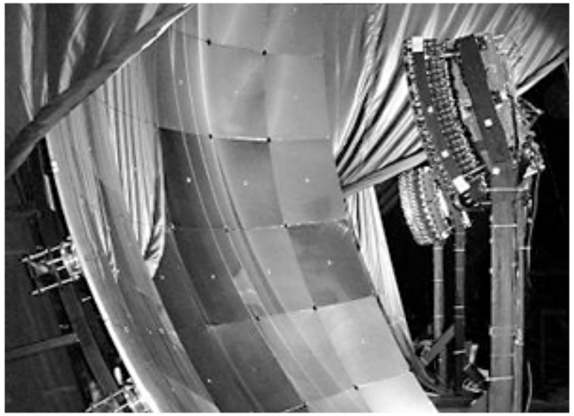

the Surface Detectors

longitudinal shower profile

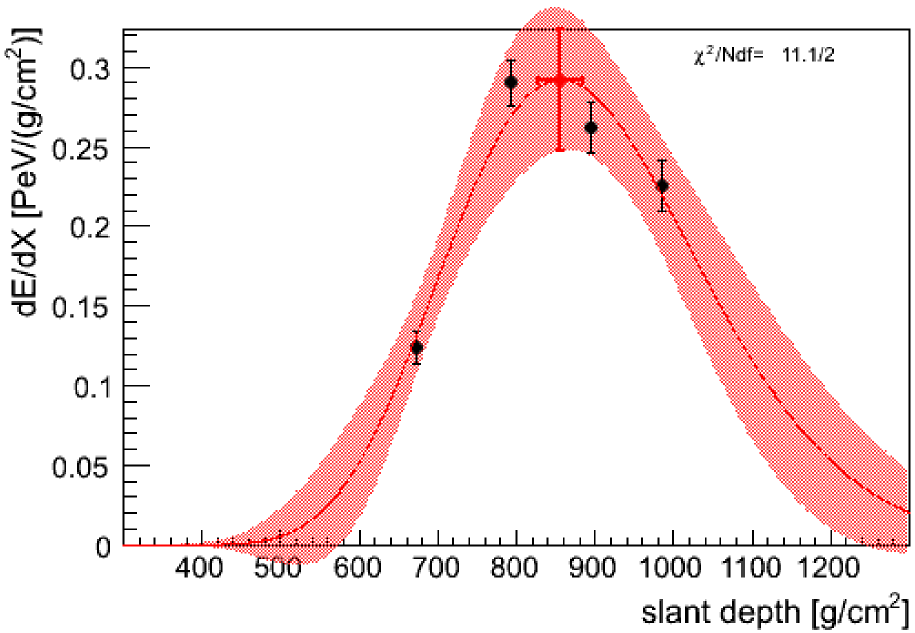

footprint

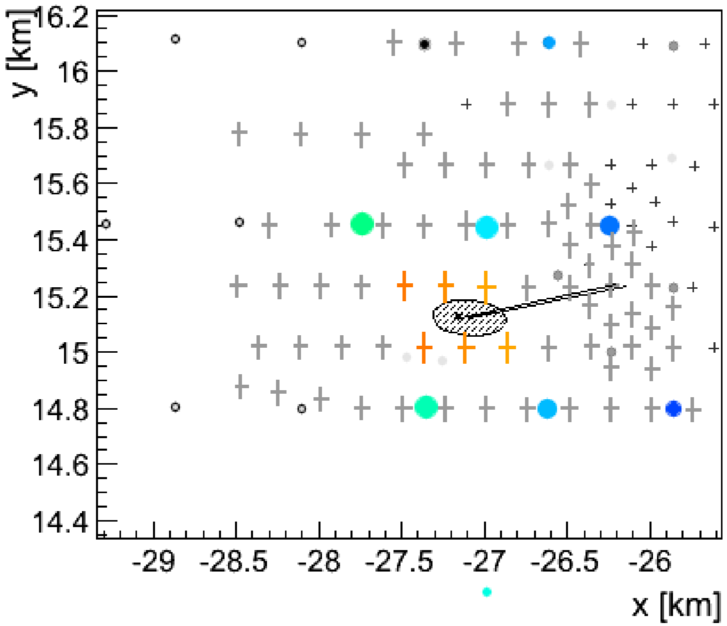

PIERRE AUGER OBSERVATORY

E ~ 2*10^{17} eV X_{max} ~ 860 g/cm² zenith angle ~ 75° azimuth angle ~ 8°

An air shower measured simultaneously with ...

the Radio Detectors

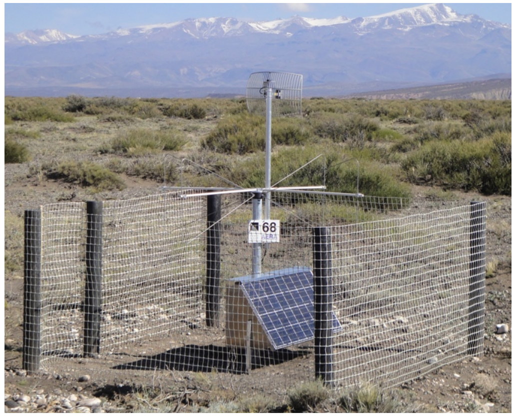

the Surface Detectors

radio pulse

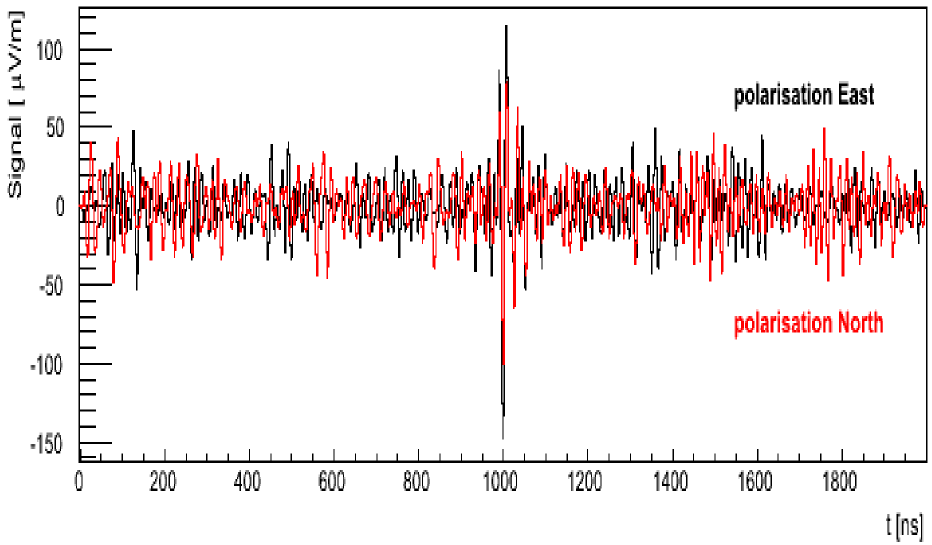

footprint

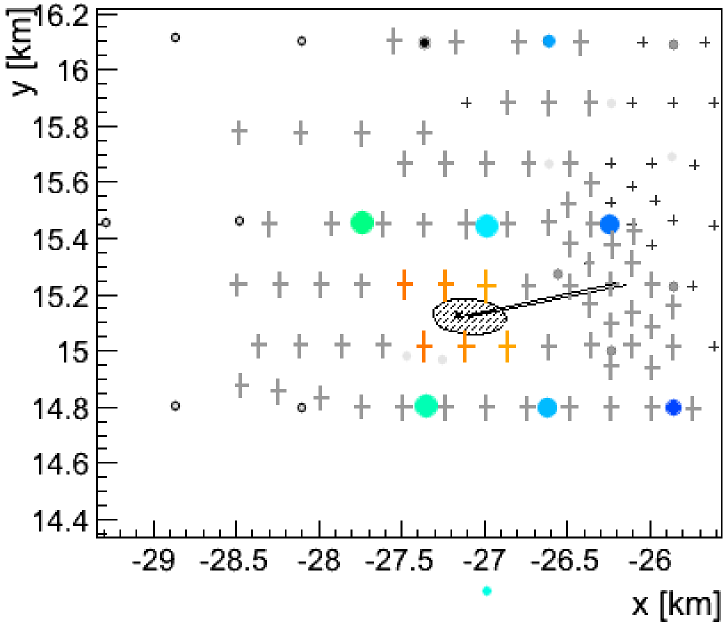

E ~ 2*10^{17} eV   X$_{max}$ ~ 860 g/cm^2 zenith angle ~ 75°   azimuth angle ~ 8°

PIERRE AUGER OBSERVATORY

An air shower measured simultaneously with ...

the Muon Detectors **the Surface Detectors**

lateral shower profile

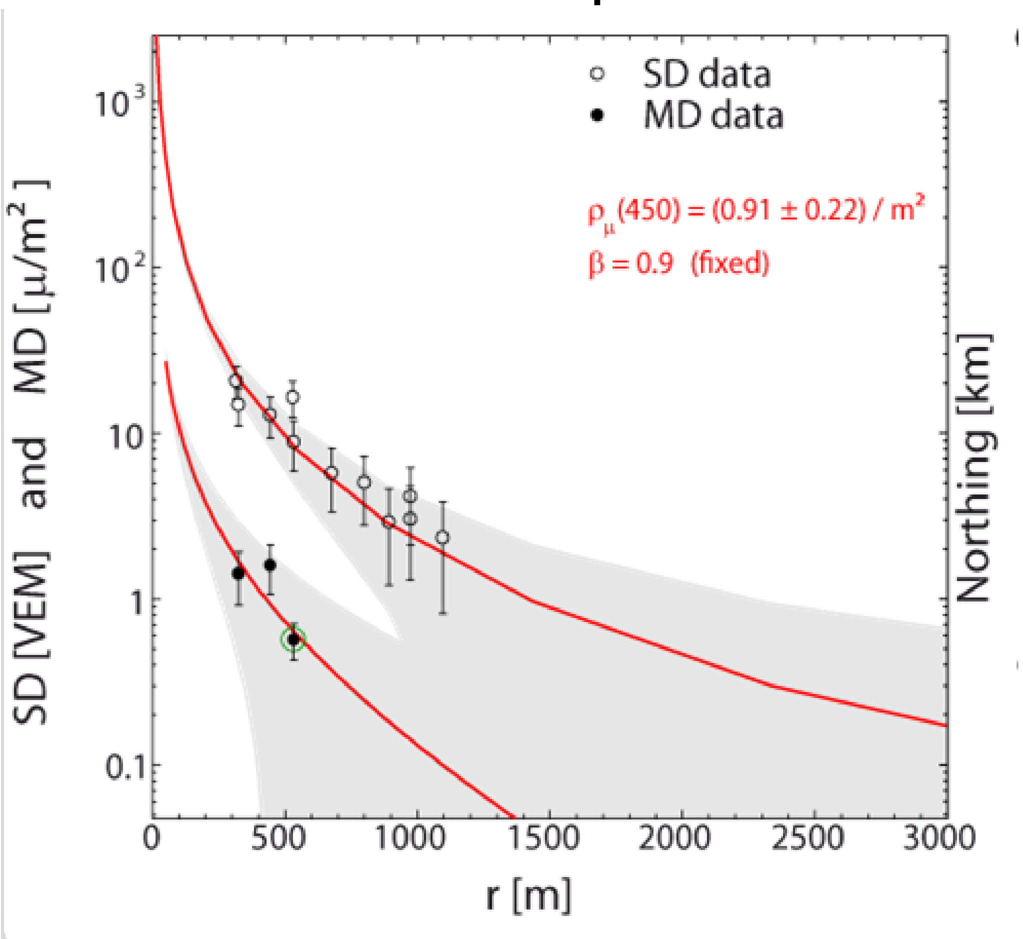

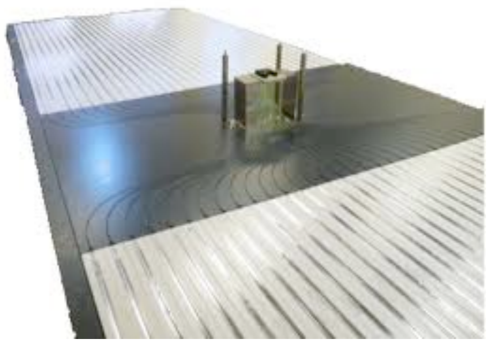

E ~ 2*10^{17} eV **X_{max} ~ 860 g/cm²** **zenith angle ~ 75°** **azimuth angle ~ 8°**

PIERRE AUGER OBSERVATORY

Polarization

Arrival direction

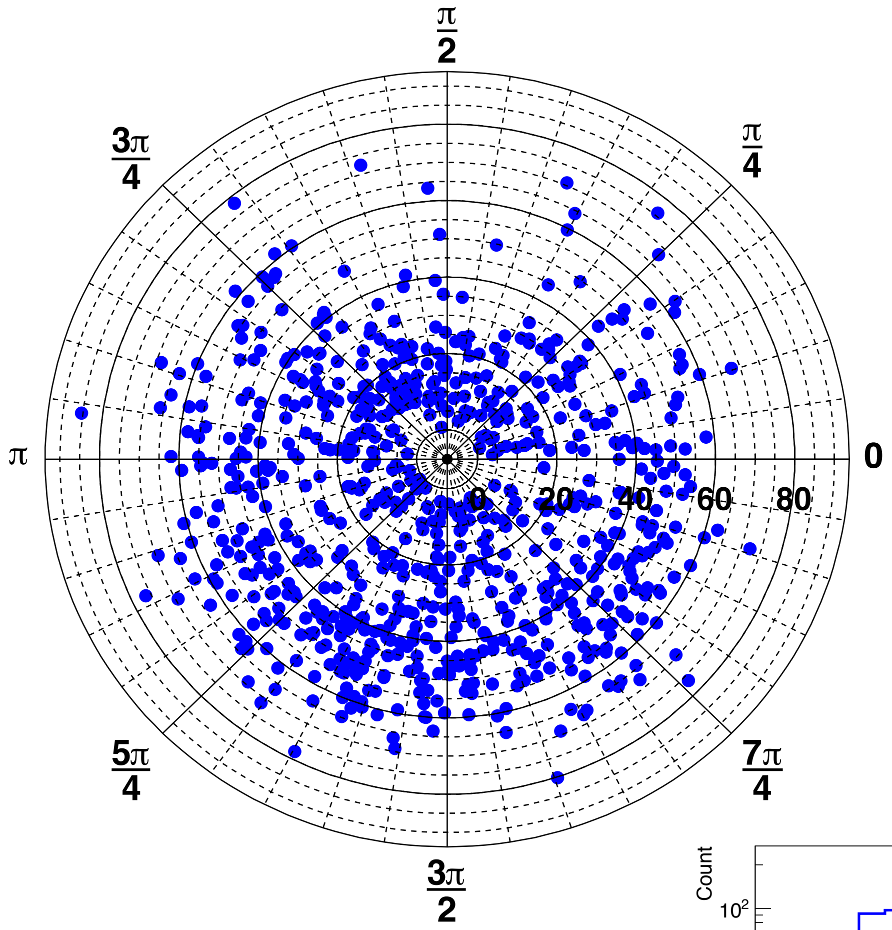

of showers with strong radio signal

north-south asymmetry
v x B effect

Geomagnetic field

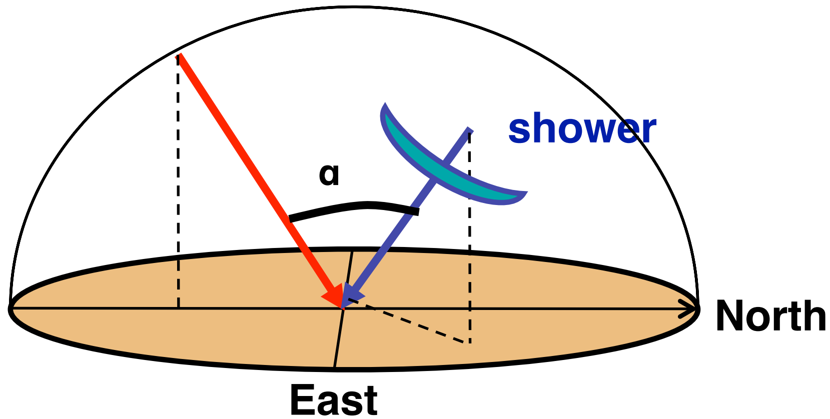

$$\vec{\epsilon} \propto \vec{v} \times \vec{B}$$

Auger Engineering Radio Array

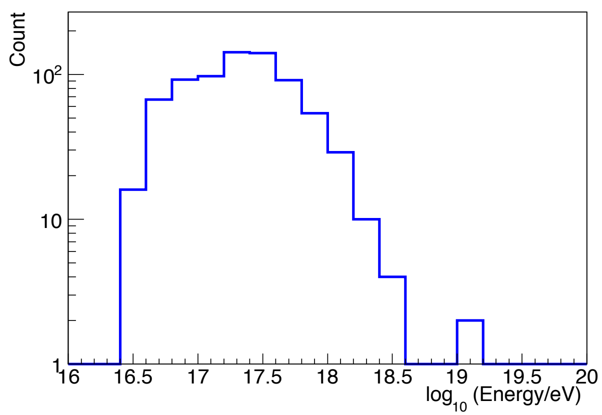

Arrival direction

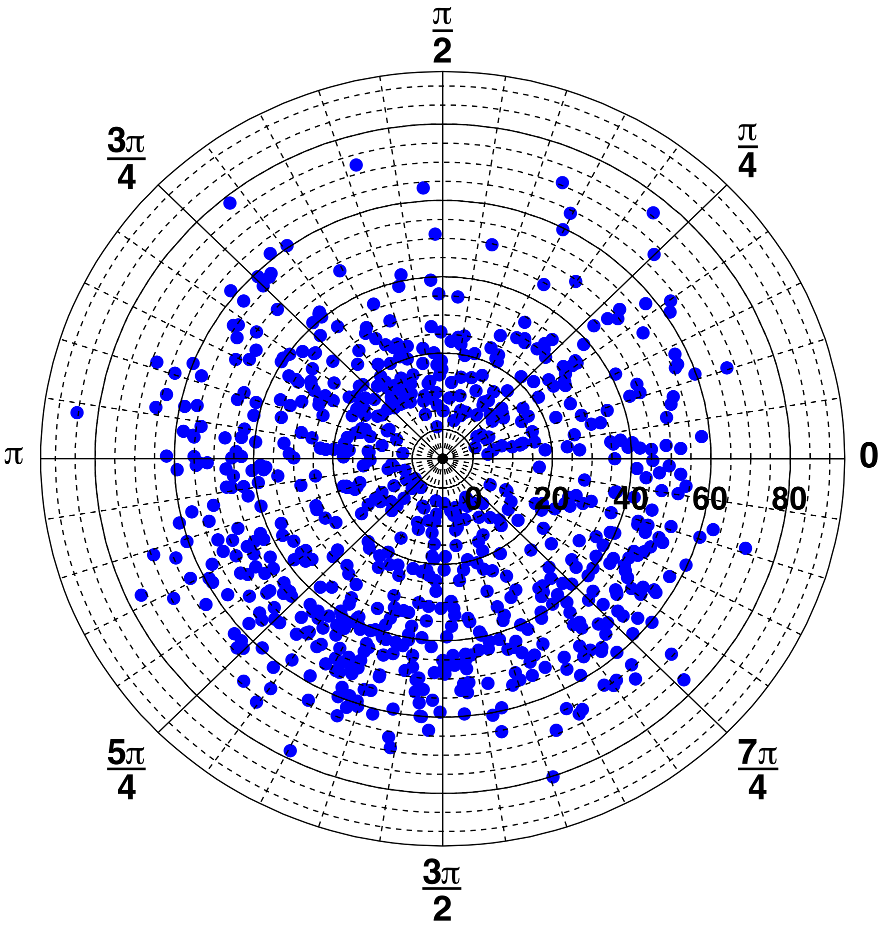

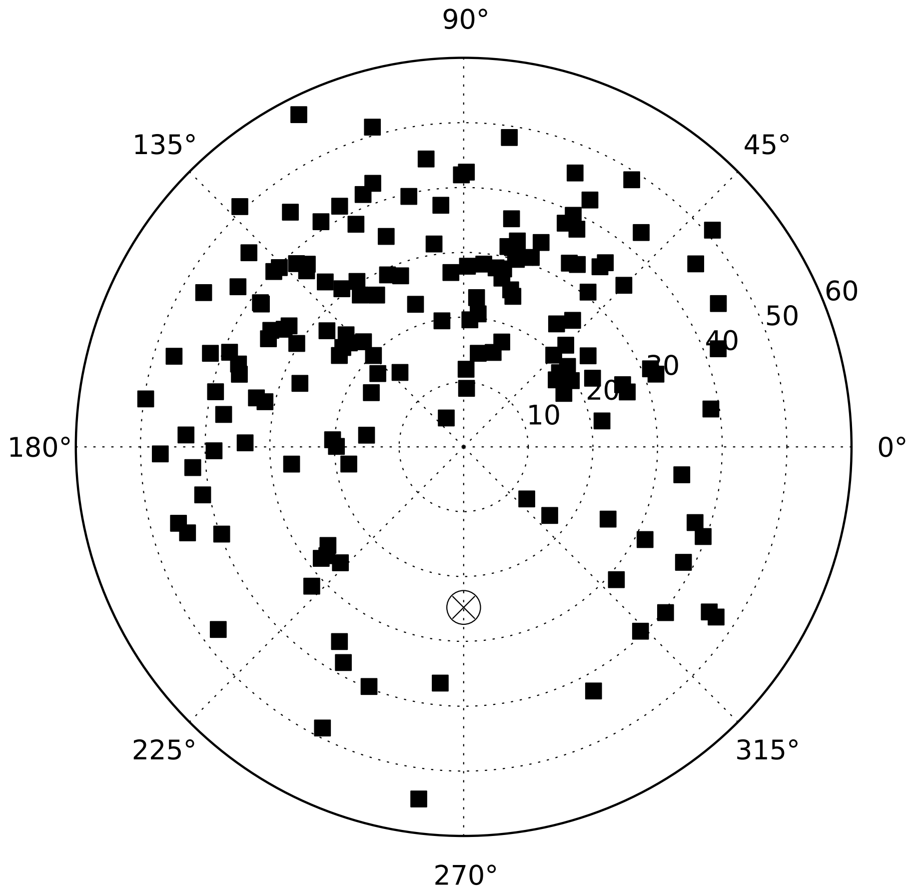

AERA
Auger Engineering Radio Array

LOFAR

Polarization of the radio signal

measure direction of electric field vector at different positions

geomagnetic **Askaryan**

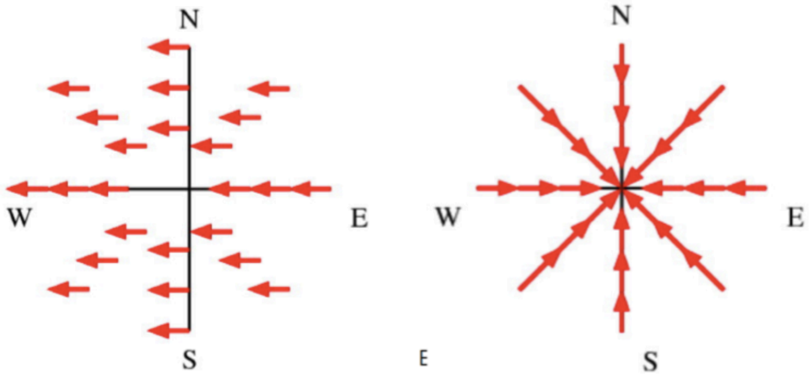

$$a \equiv \sin(\alpha) \frac{|E^{A}|}{|E^{G}|}.$$

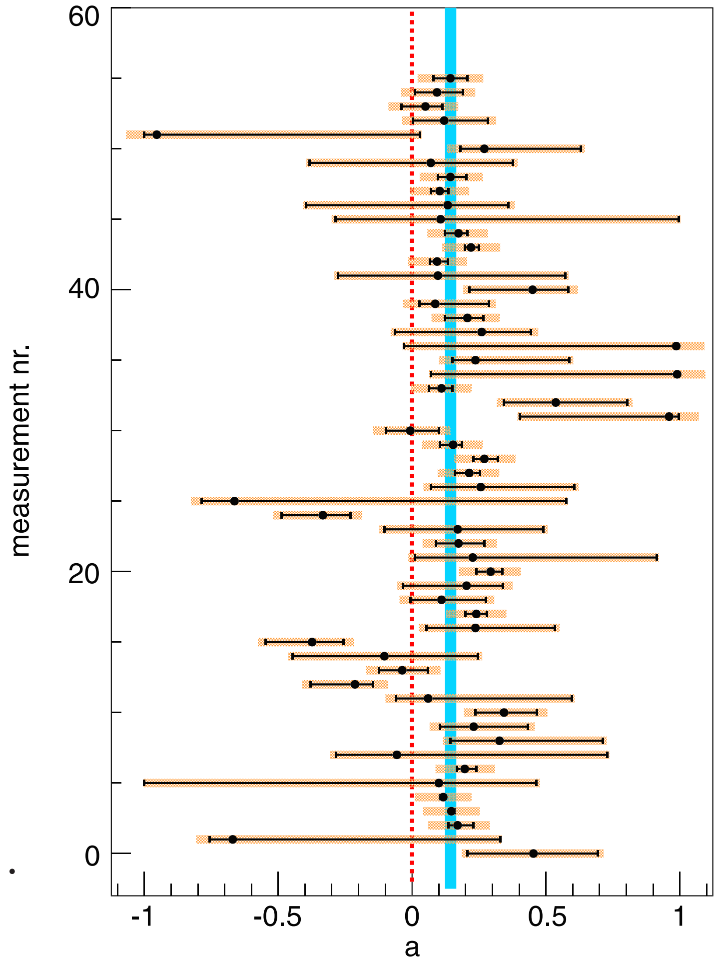

FIG. 9 (color online). Distribution of most probable values of a [see Eq. (10)] and their uncertainties for the AERA24 data set (see Appendix B for details). The 68% confidence belt around the mean value of a is shown as the solid blue line; the value $a = 0$ is indicated with the dotted red line; see text for further details.

emission dominated by geomagnetic emission
14 +/- 2 % charge excess processes

A. Aab et al, Phys. Rev. D 89 (2014) 052002

Polarization footprint
of an individual air shower

geomagnetic

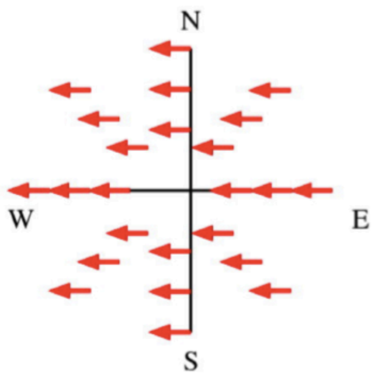

Askaryan

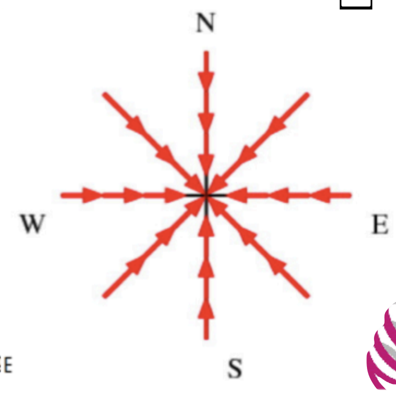

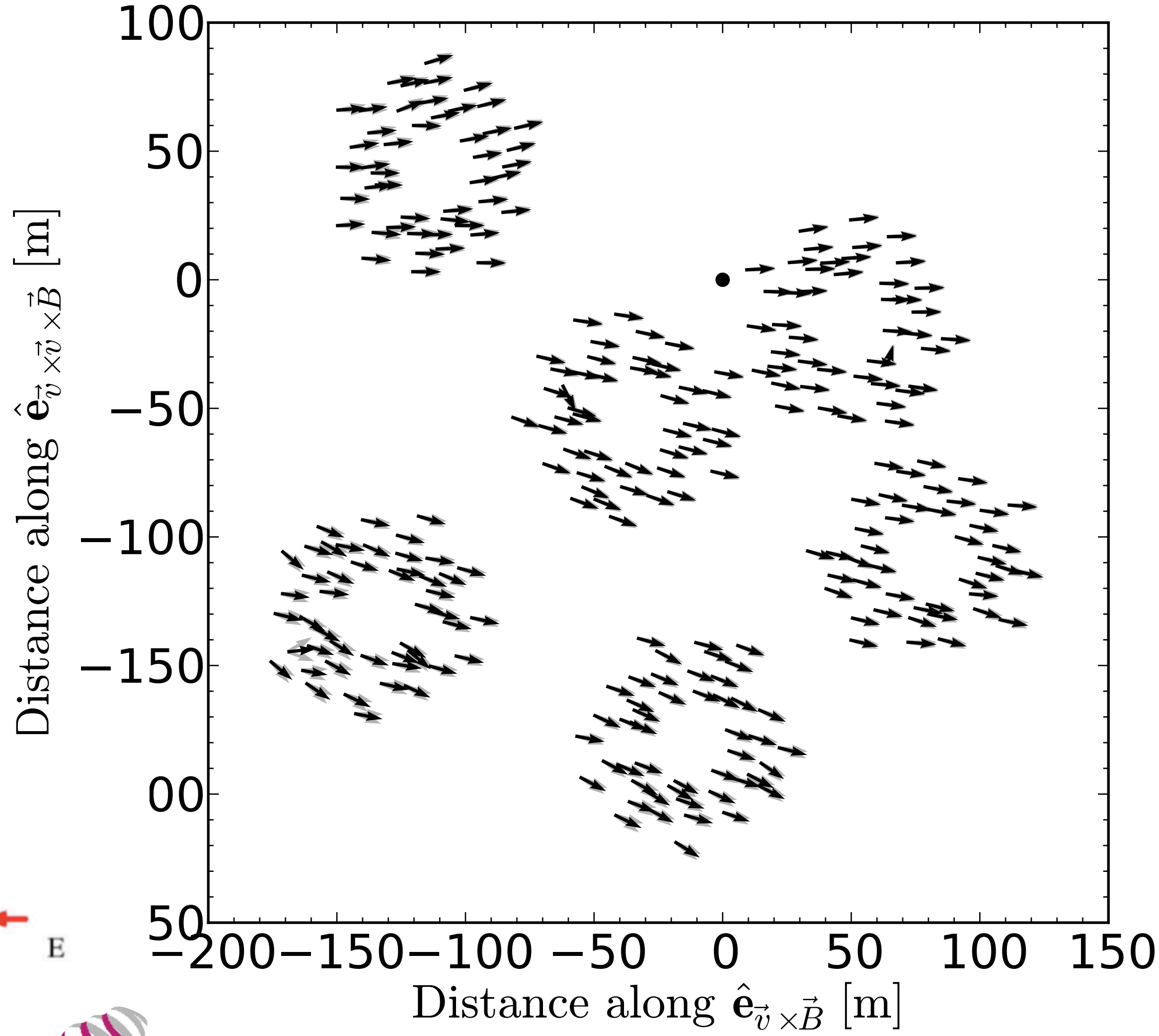

LOFAR

JCAP in press, arXiv:1406.1355

Charge excess fraction

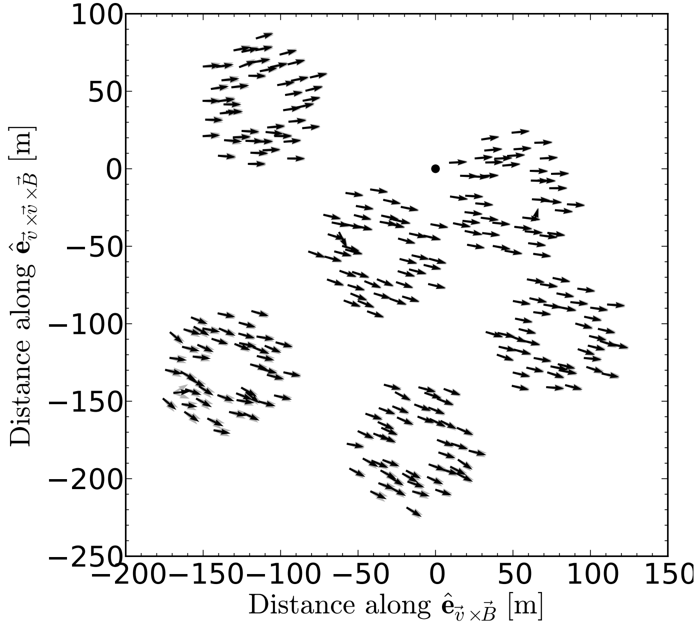

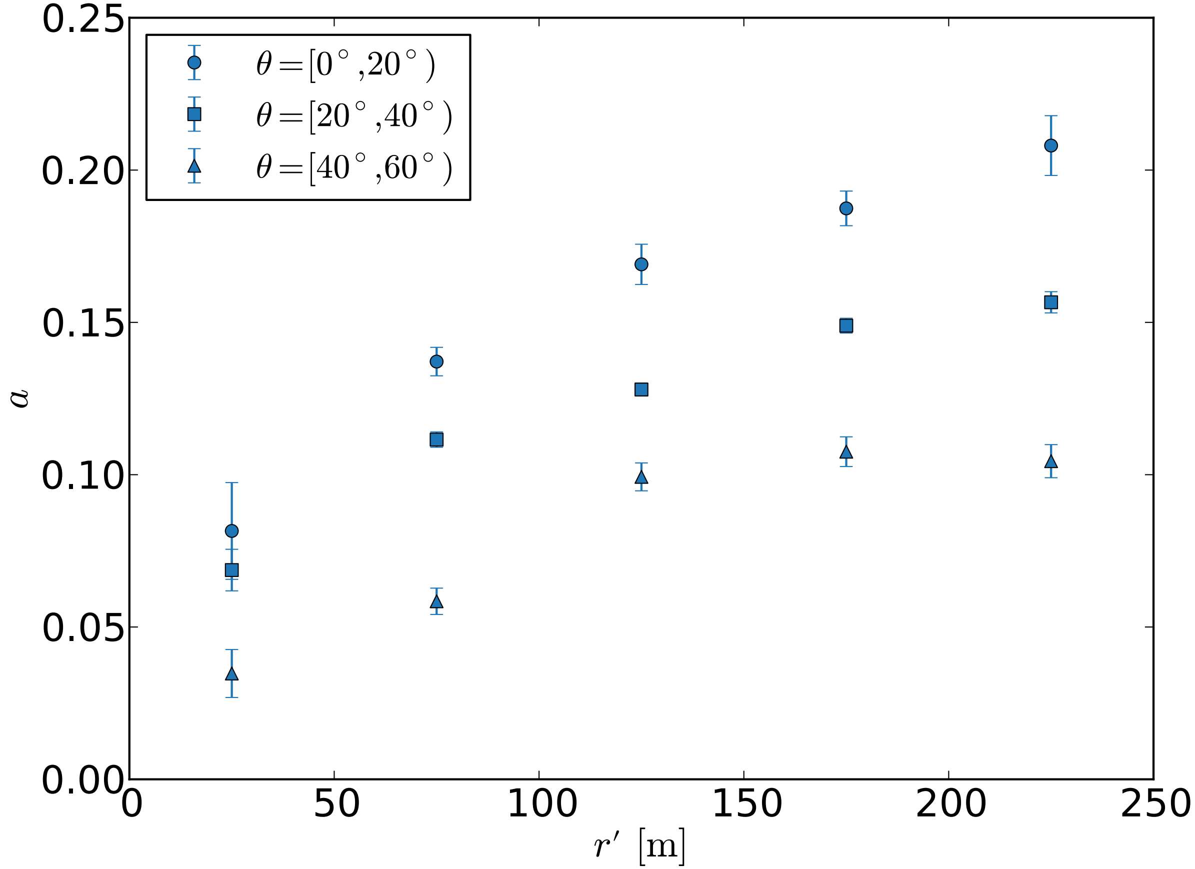

geomagnetic **Askaryan**

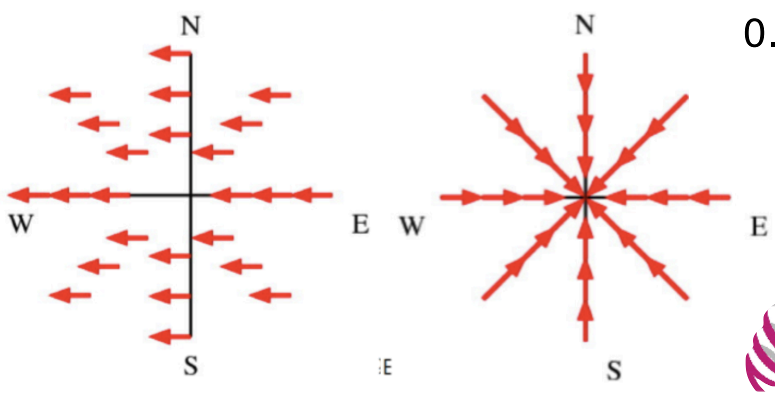

LOFAR

JCAP in press, arXiv:1406.1355

Lateral Distribution

Lateral distribution of radio signals

as measured by LOFAR

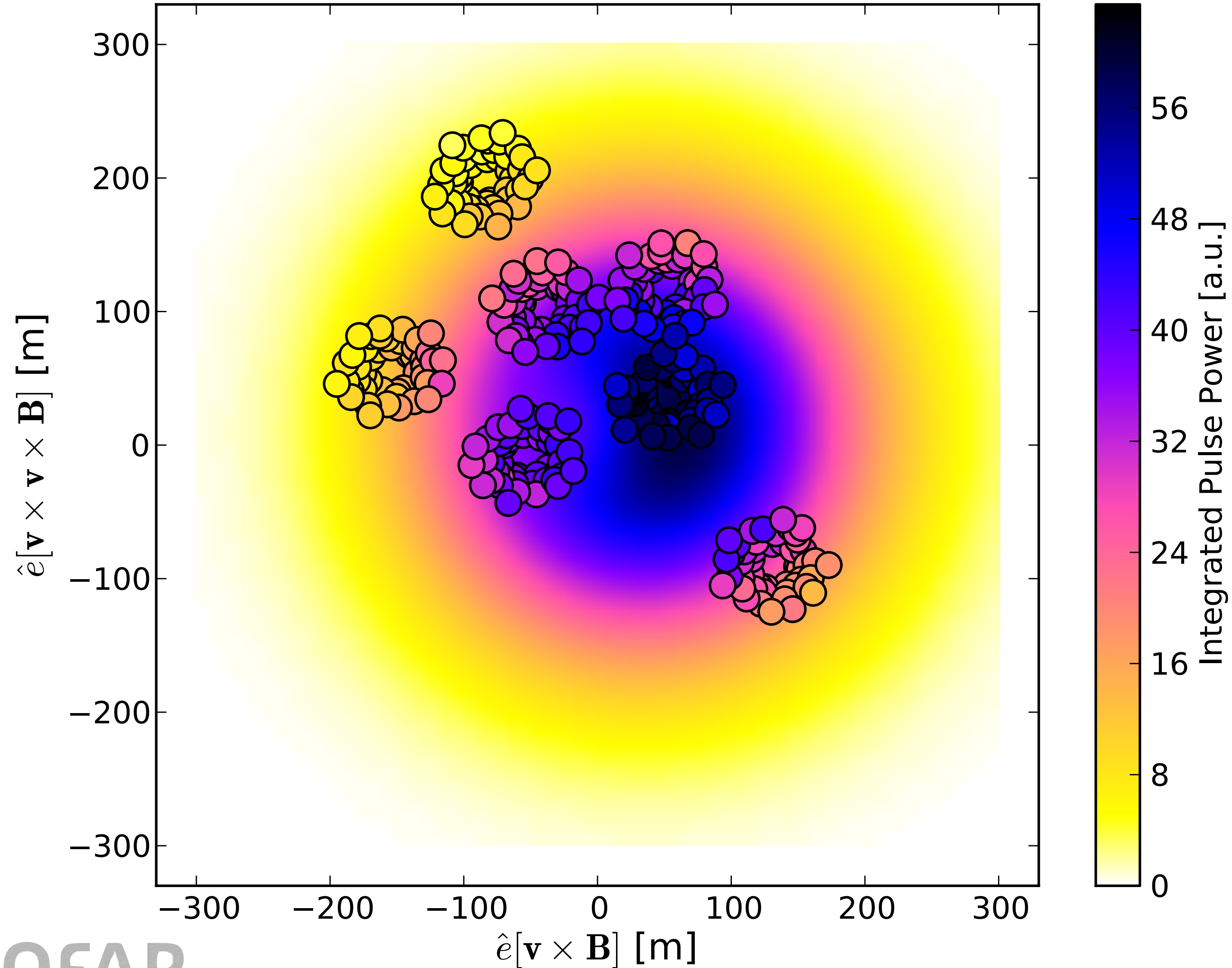

LOFAR

A. Nelles et al., Astropart. Phys. 60 (2015) 13

Lateral distribution of radio signals

as measured by LOFAR

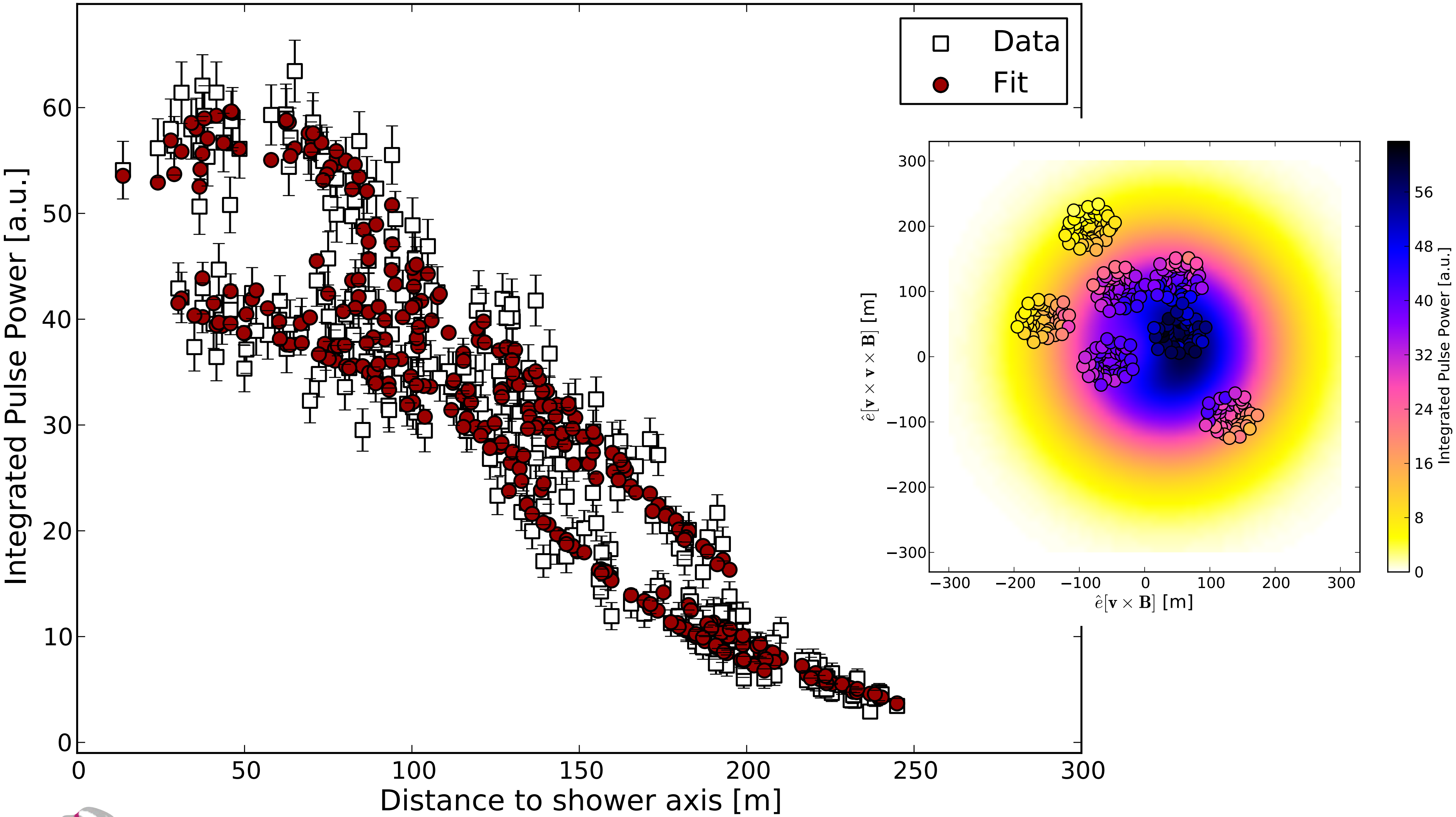

LOFAR

A. Nelles et al., Astropart. Phys. 60 (2015) 13

Lateral distribution of radio signals

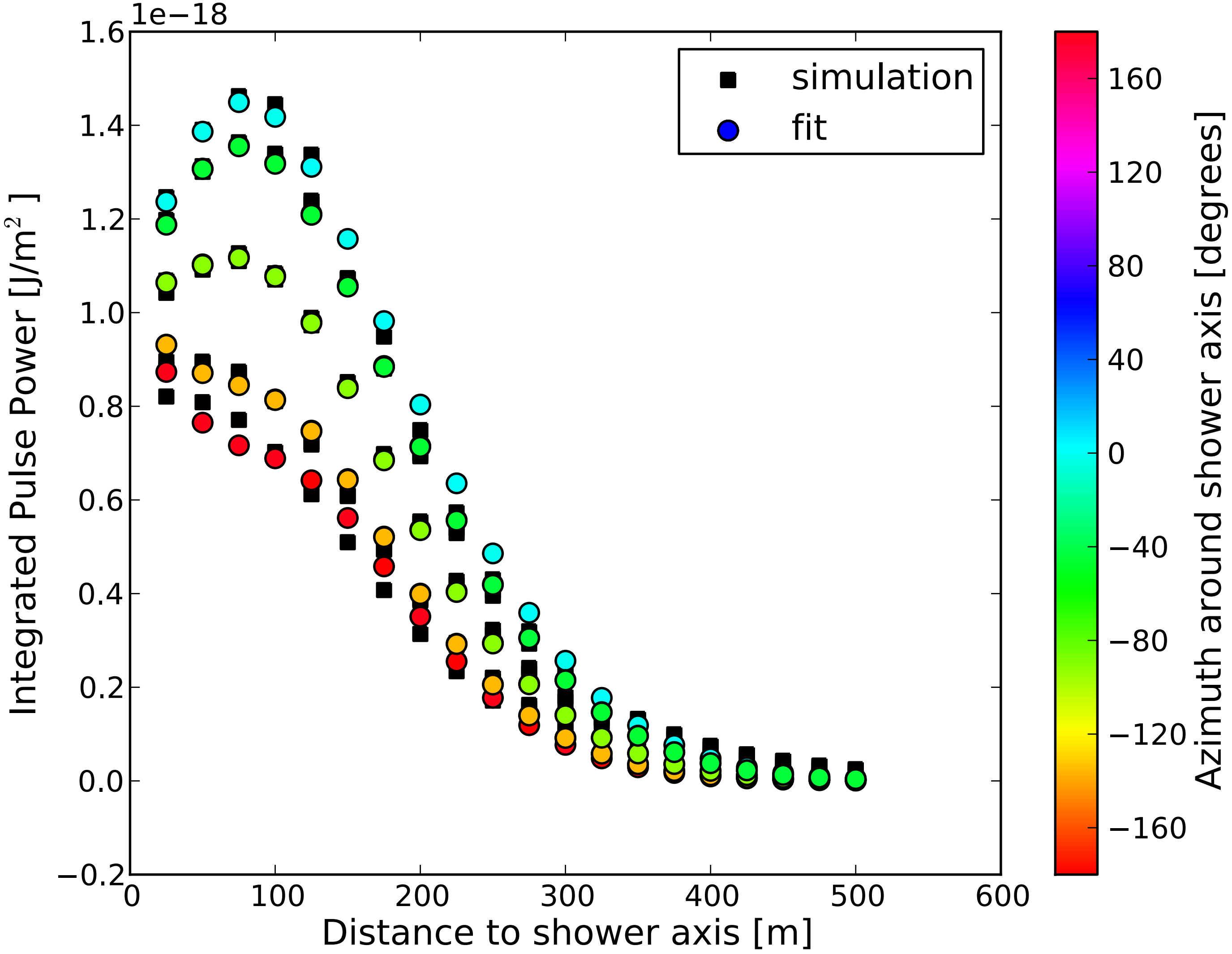

Lateral distribution of radio signals

not rotational symmetric

fit two Gaussian functions

$$P(x',y') = A_+ \cdot \exp\left(\frac{-[(x'-X_+)^2+(y'-Y_+)^2]}{\sigma_+^2}\right) - A_- \cdot \exp\left(\frac{-[(x'-X_-)^2+(y'-Y_-)^2]}{\sigma_-^2}\right) + O$$

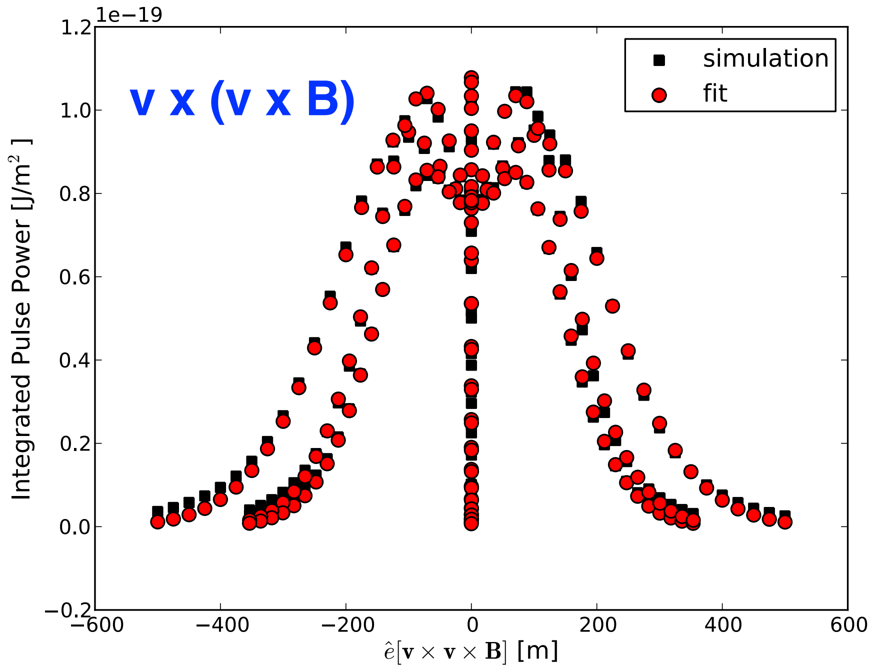

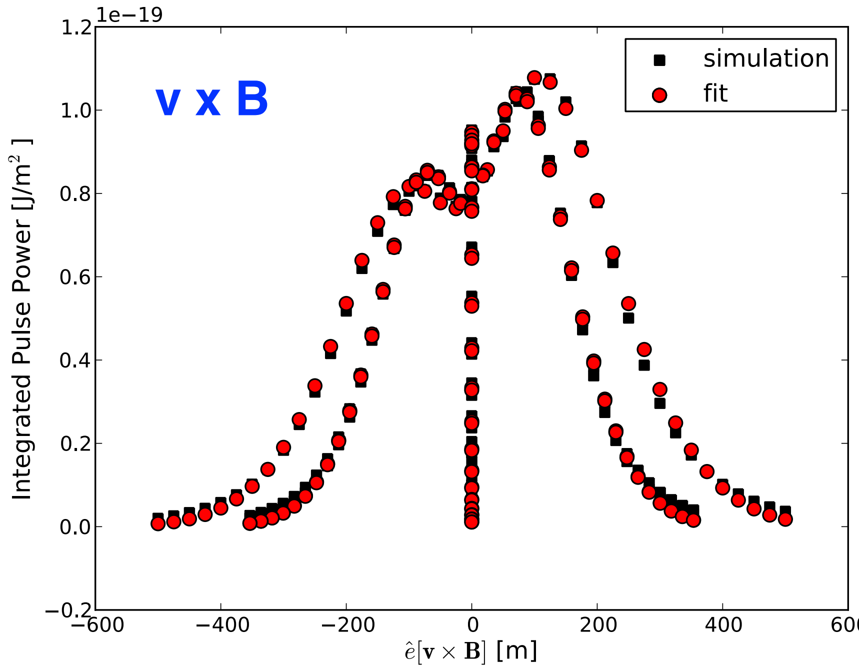

A. Nelles et al., Astropart. Phys. 60 (2015) 13

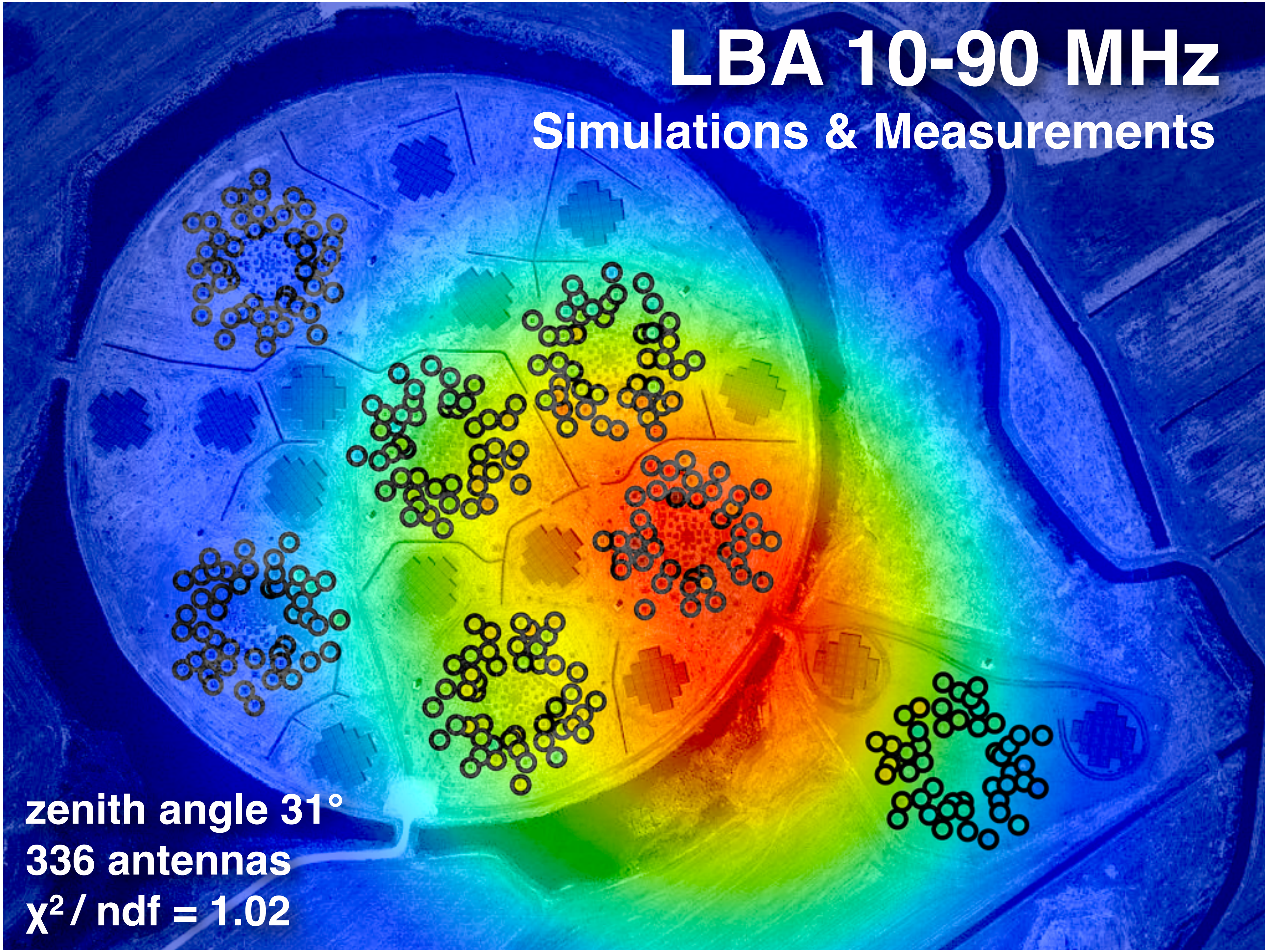
LBA 10-90 MHz
Simulations & Measurements
zenith angle 31°
336 antennas
χ² / ndf = 1.02

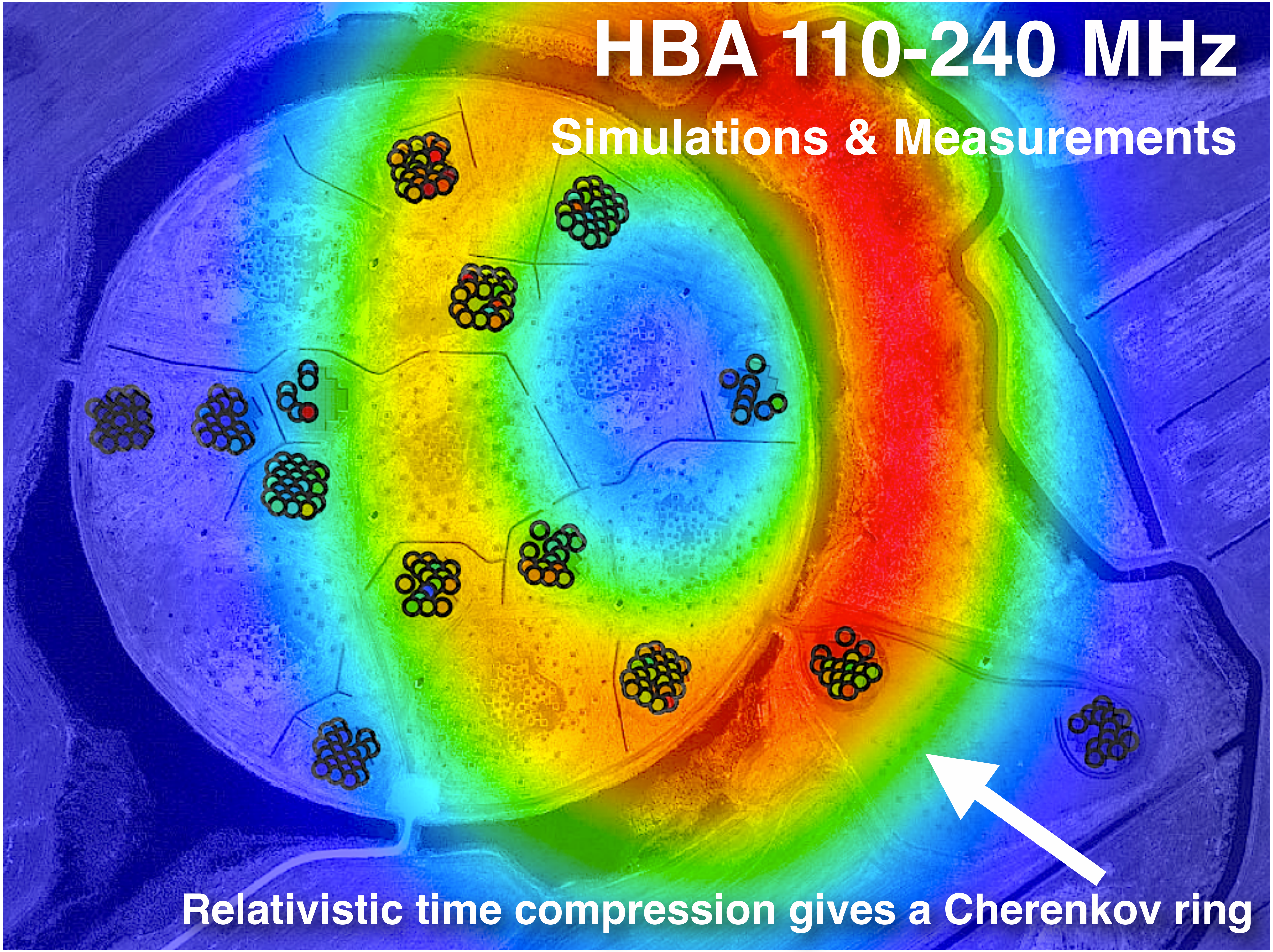
HBA 110-240 MHz
Simulations & Measurements
Relativistic time compression gives a Cherenkov ring

Radio emission at 120 - 240 MHz

- **LOFAR is the only dedicated experiment with high-band antennas**
  - **tuned to astronomical observations**
  - **include analogue beamforming**
  - **complicated calibration routine**

- **Signals expected to be**
  - **more affected by Cherenkov enhancement**
  - **concentrated on a ring of emission**

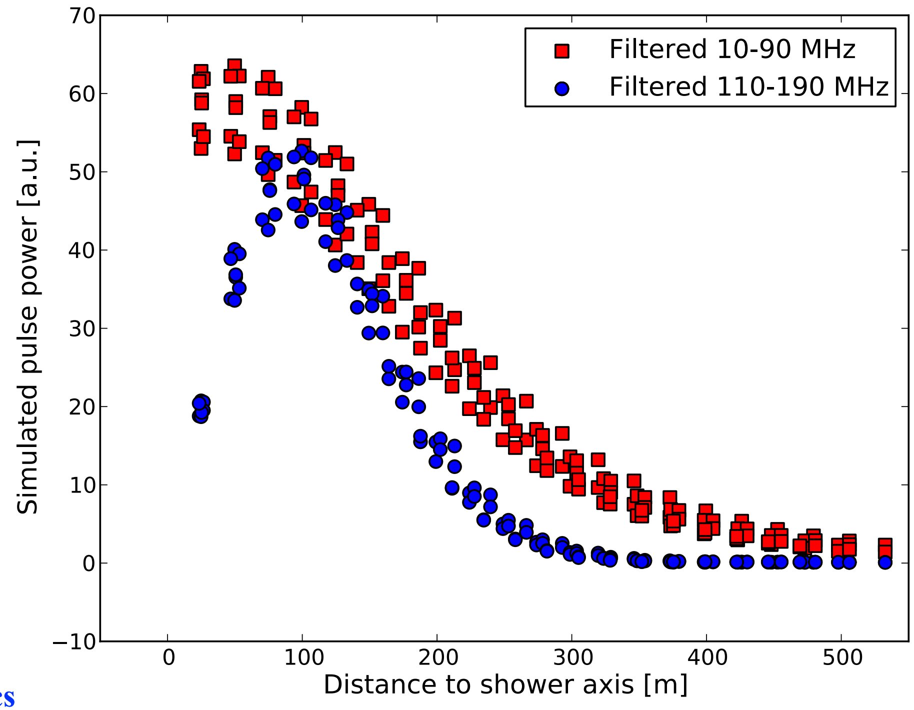

A. Nelles et al (LOFAR Collaboration), subm. to Astroparticle Physics

Measuring Cherenkov Rings

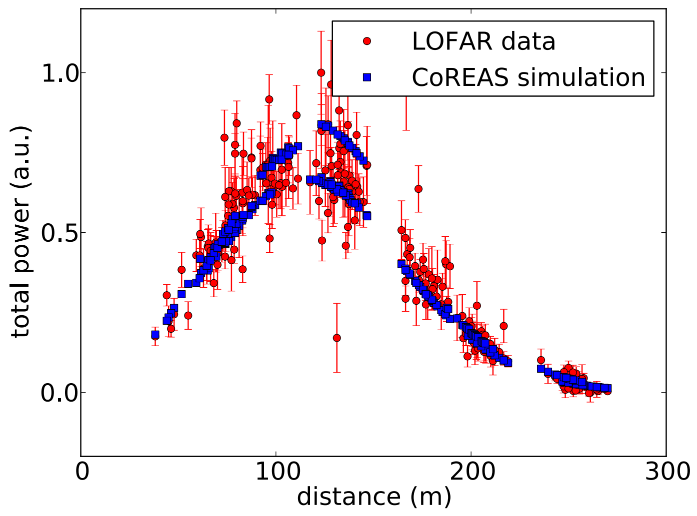

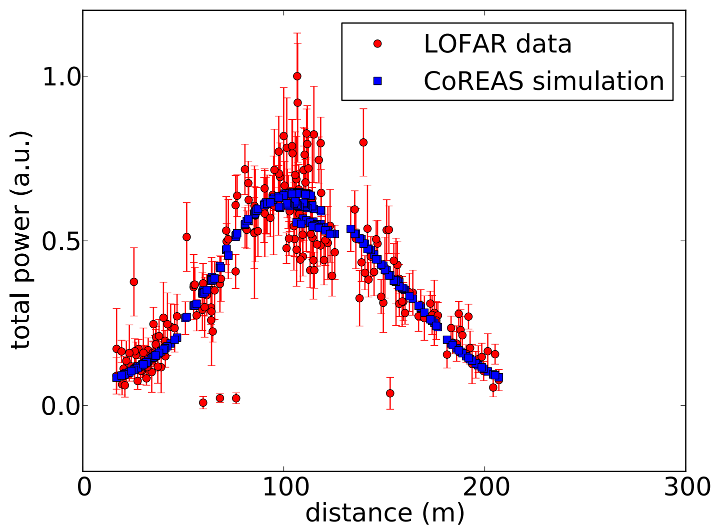

110 - 190 MHz

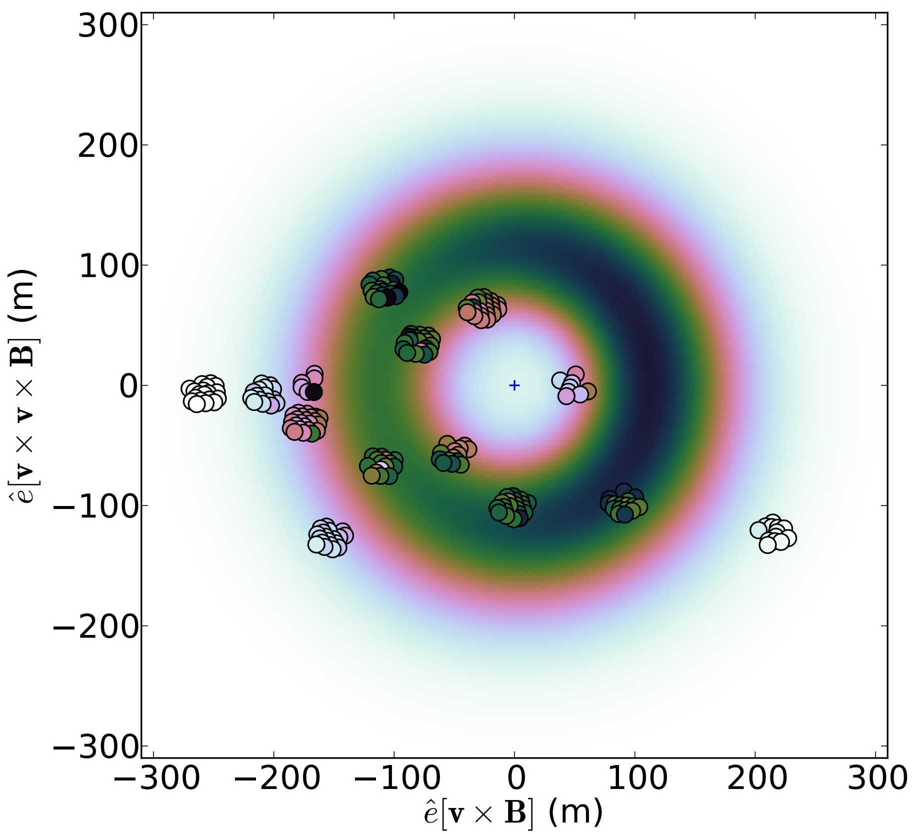

- **higher frequency-range: dominance of relativistic time-compression**
- **first experiment to observe these in single events**

A. Nelles et al (LOFAR Collaboration), subm. to Astroparticle Physics

Direction

Shape of the Shower Front

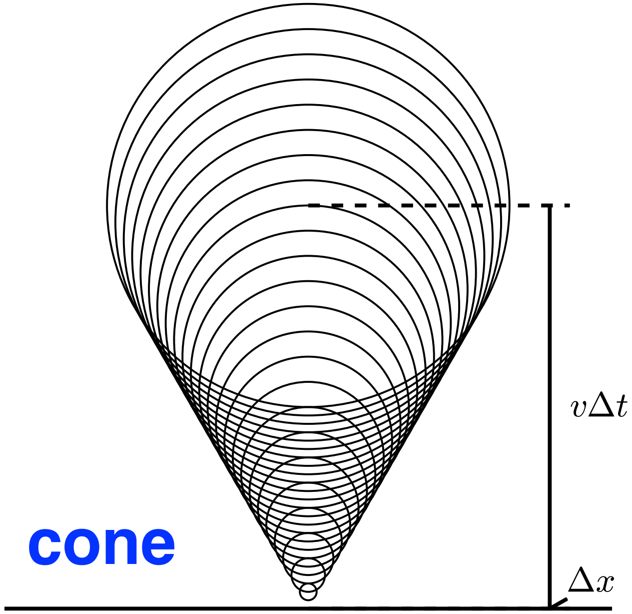

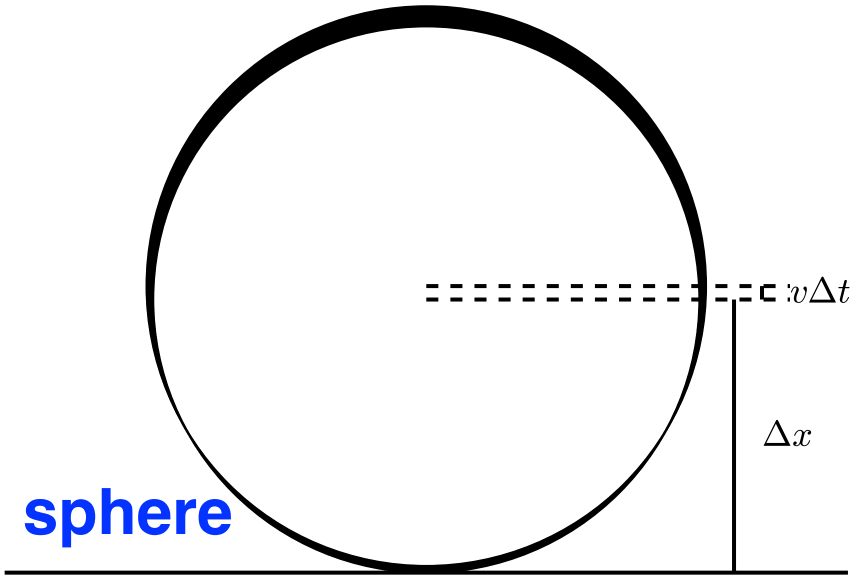

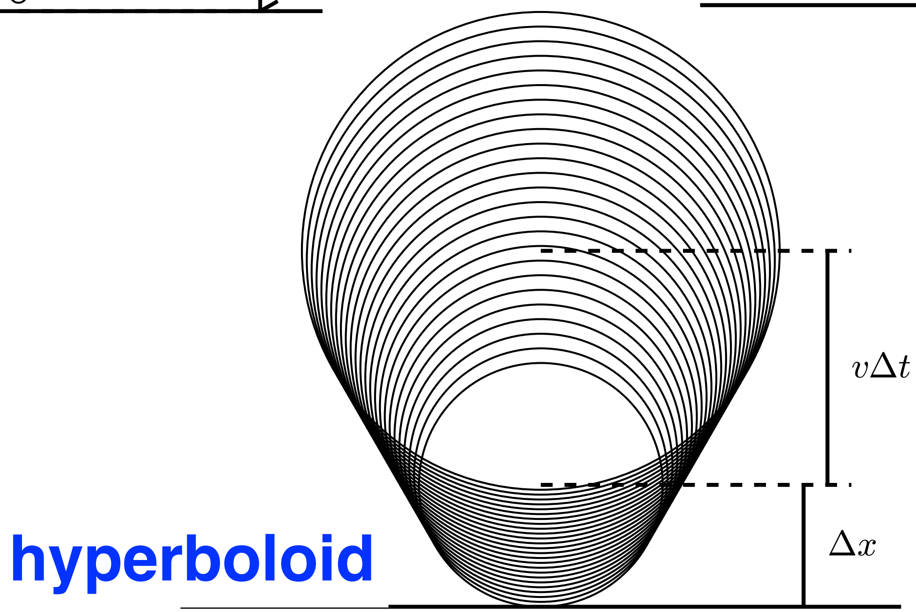

Arrival time of radio signals

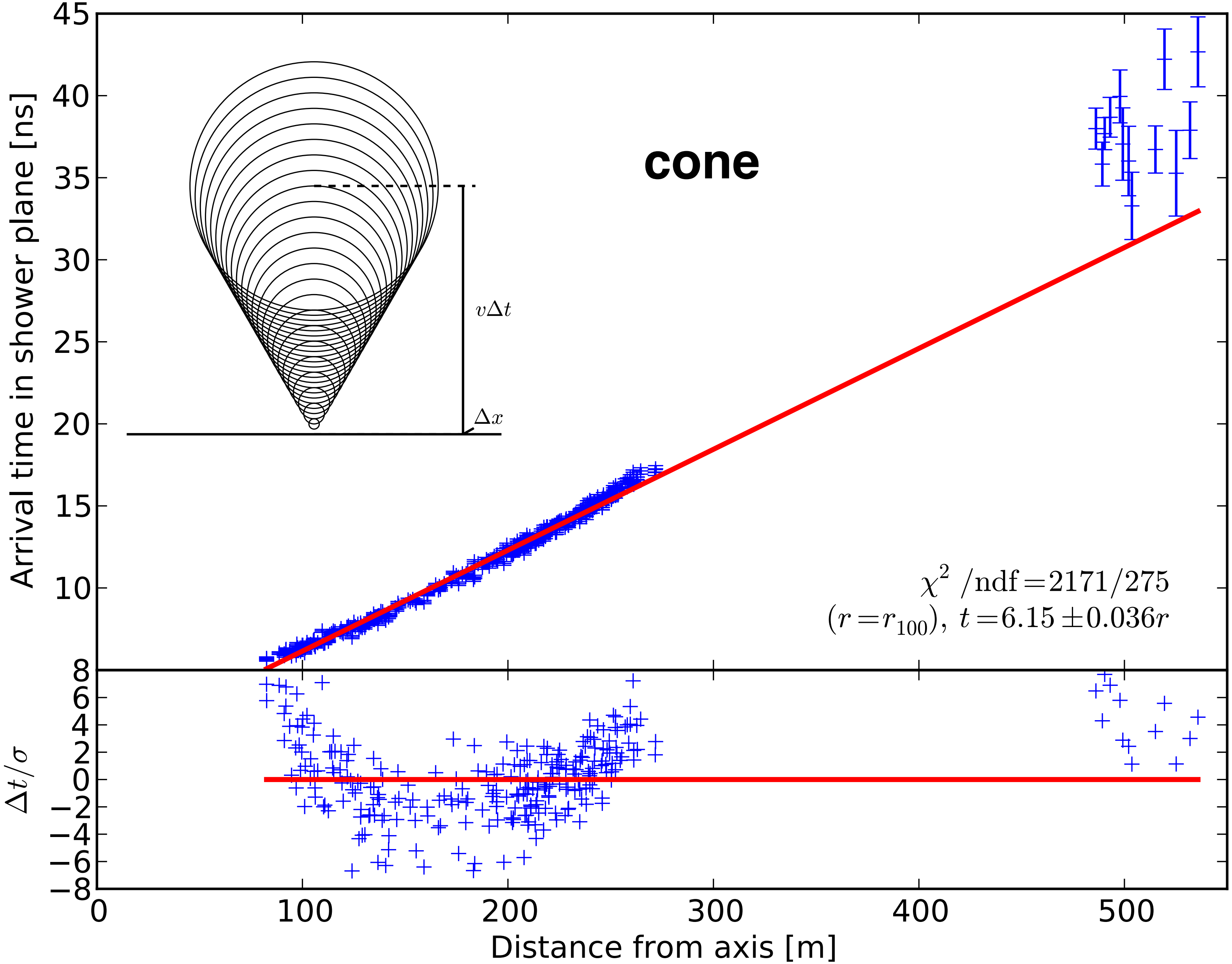

A. Corstantje et al., Astropart. Phys. 61 (2015) 22

Arrival time of radio signals

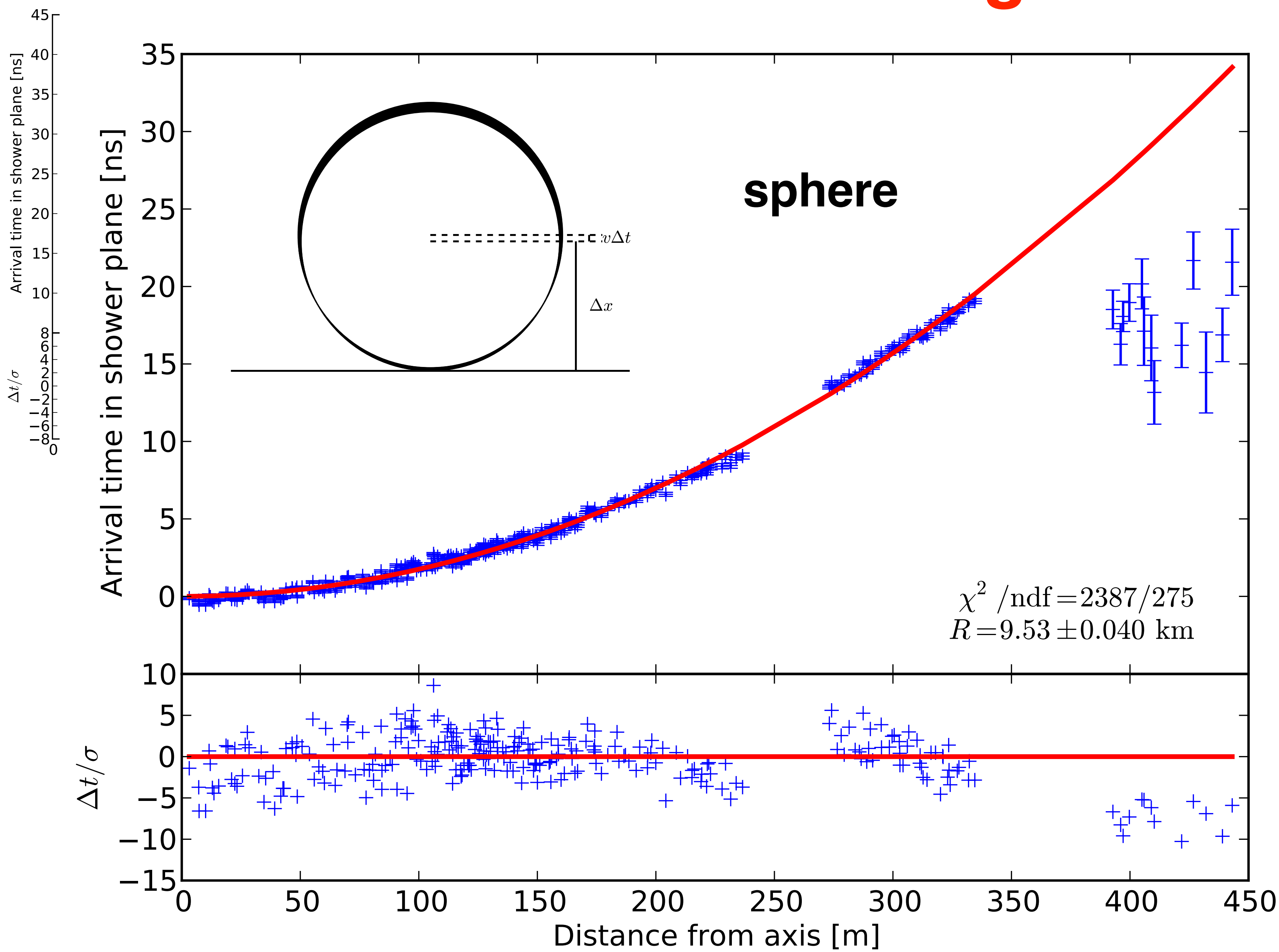

A. Corstantje et al., Astropart. Phys. 61 (2015) 22

Arrival time of radio signals

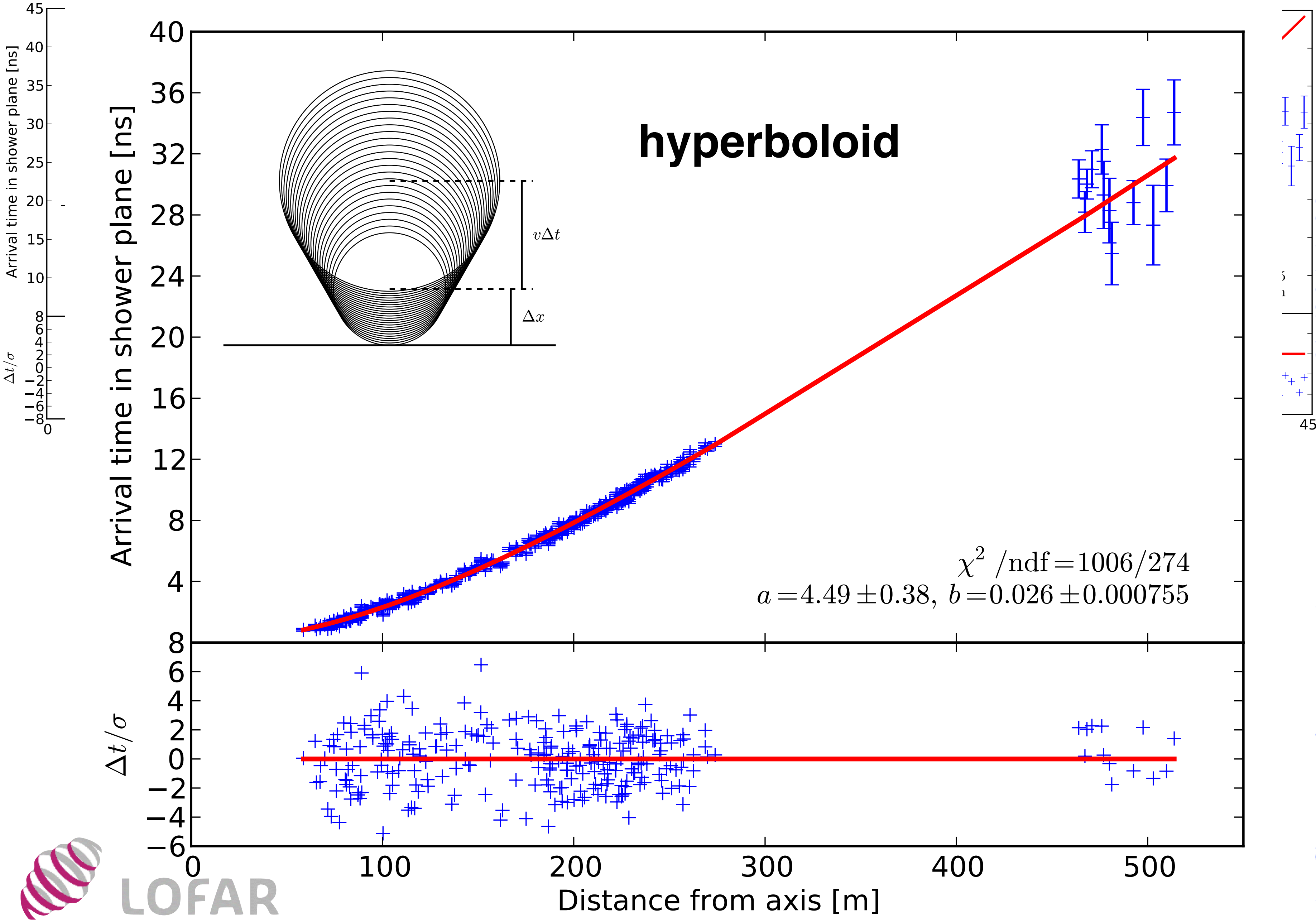

A. Corstantje et al., Astropart. Phys. 61 (2015) 22

LOFAR

Shape of Shower Front

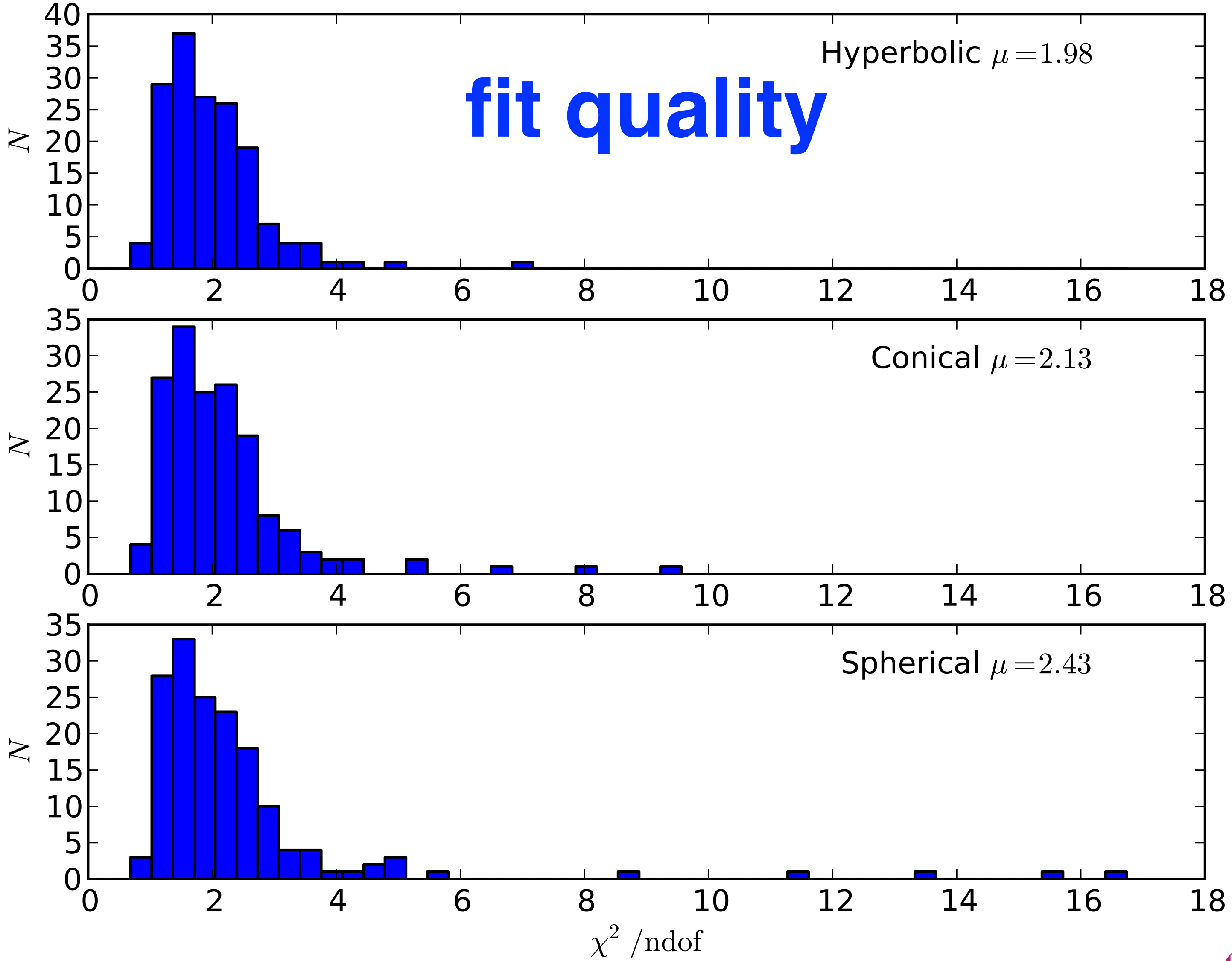

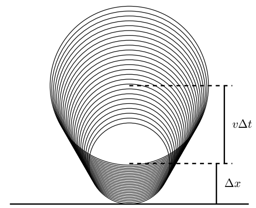

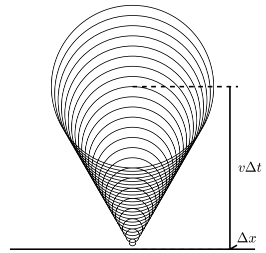

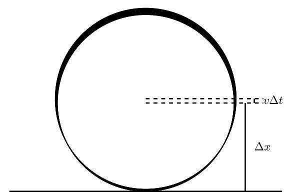

A. Corstantje et al., Astropart. Phys. 61 (2015) 22

LOFAR

Accuracy of Shower Direction

angular difference between..

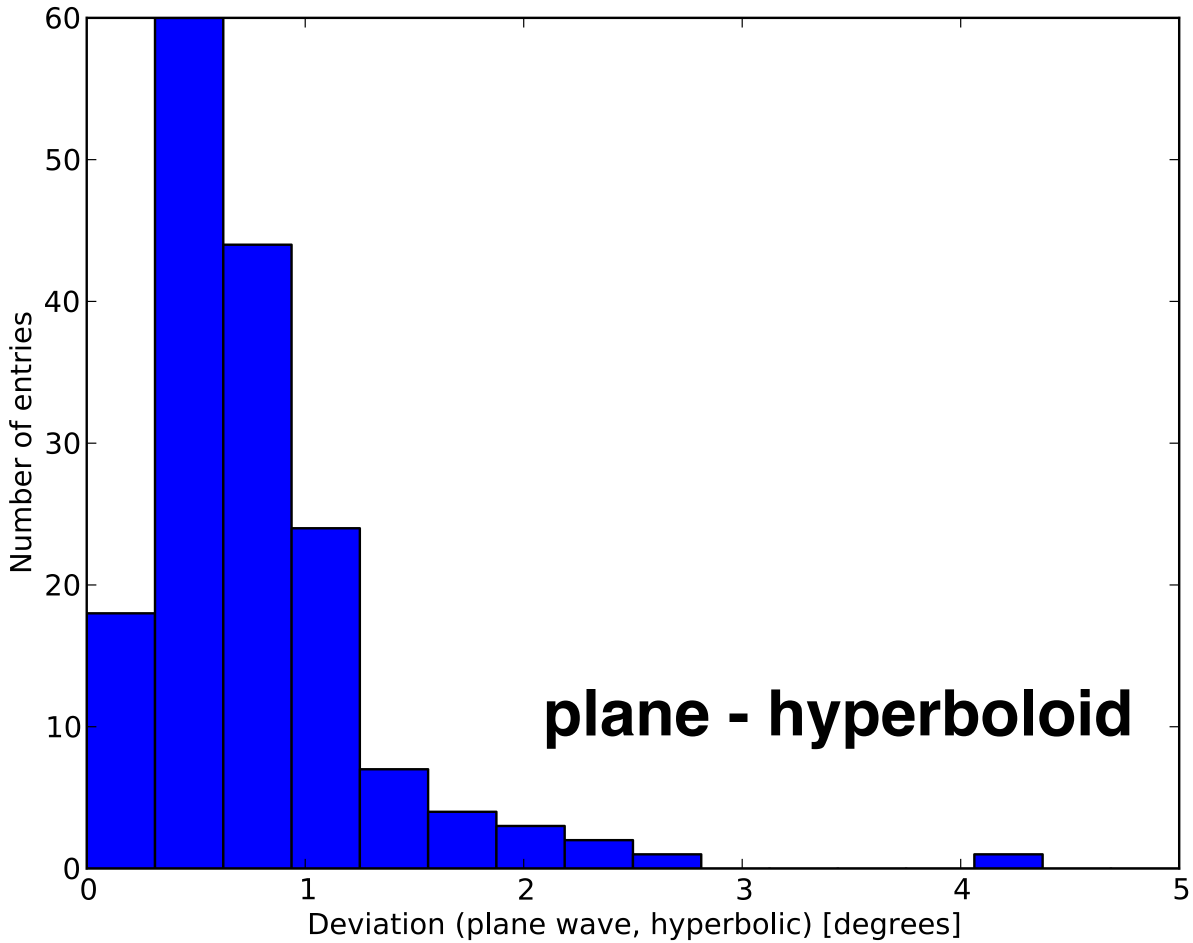

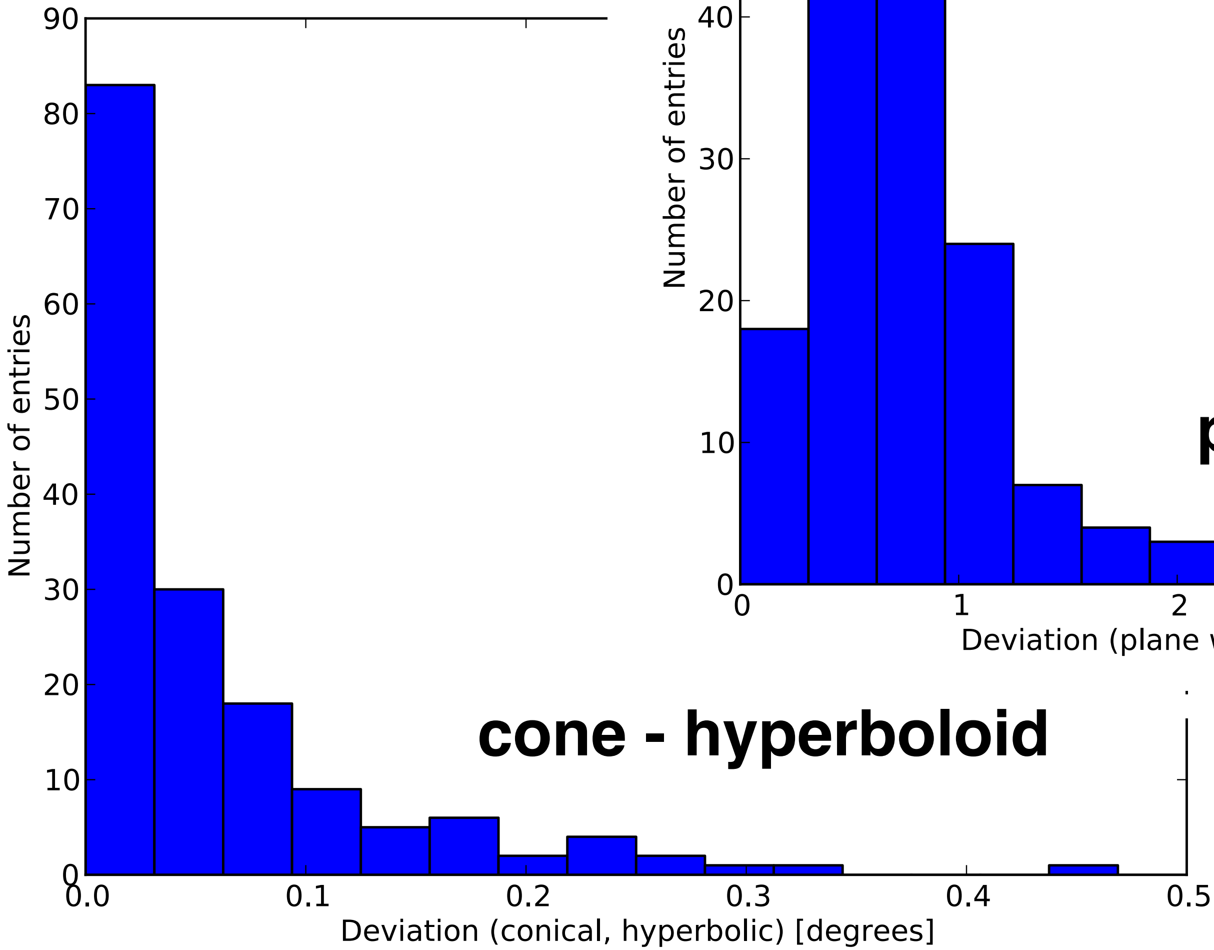

Energy

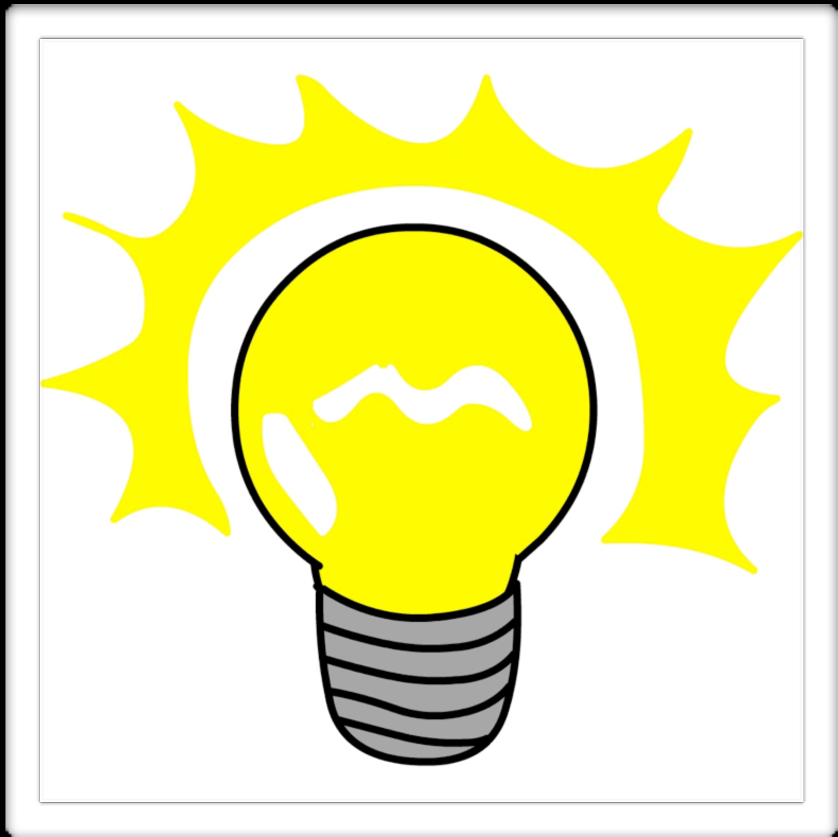

AERA: direction of E field vector

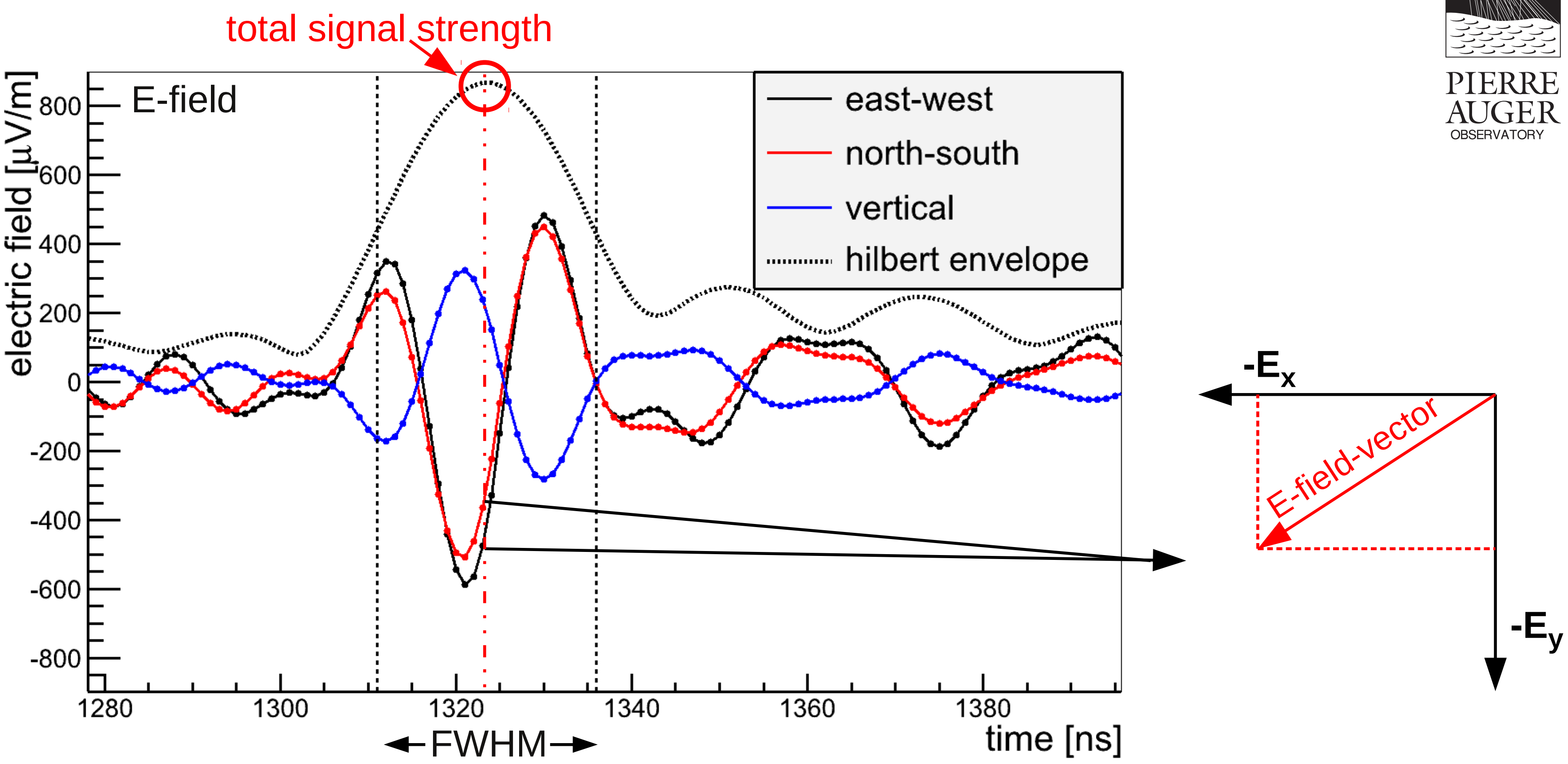

C. Glaser, ARENA (2012)

AERA: direction of E field vector

- event selection:
  - ≥ 3 self-triggered stations
  - zenith < 55°
  - no events during thunderstorms

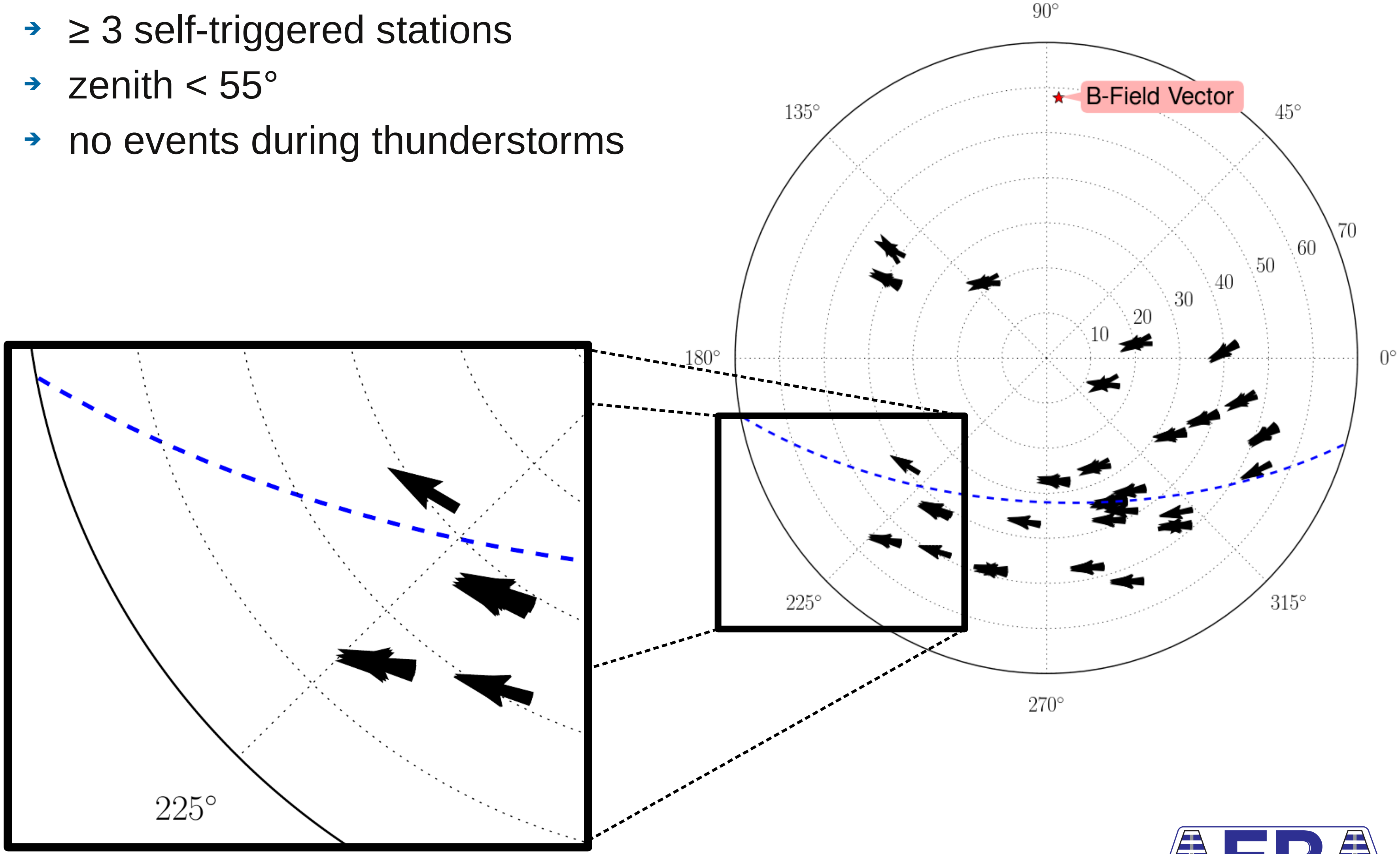

C. Glaser, ARENA (2012)

AERA Auger Engineering Radio Array

AERA: measured vs. expected values

- electric field is strongly polarised
- geomagnetic emission is dominant
  - correct electric field amplitude for incoming direction
  - $E_{scaled} = \frac{|\vec{E}|}{sin(\alpha)}$

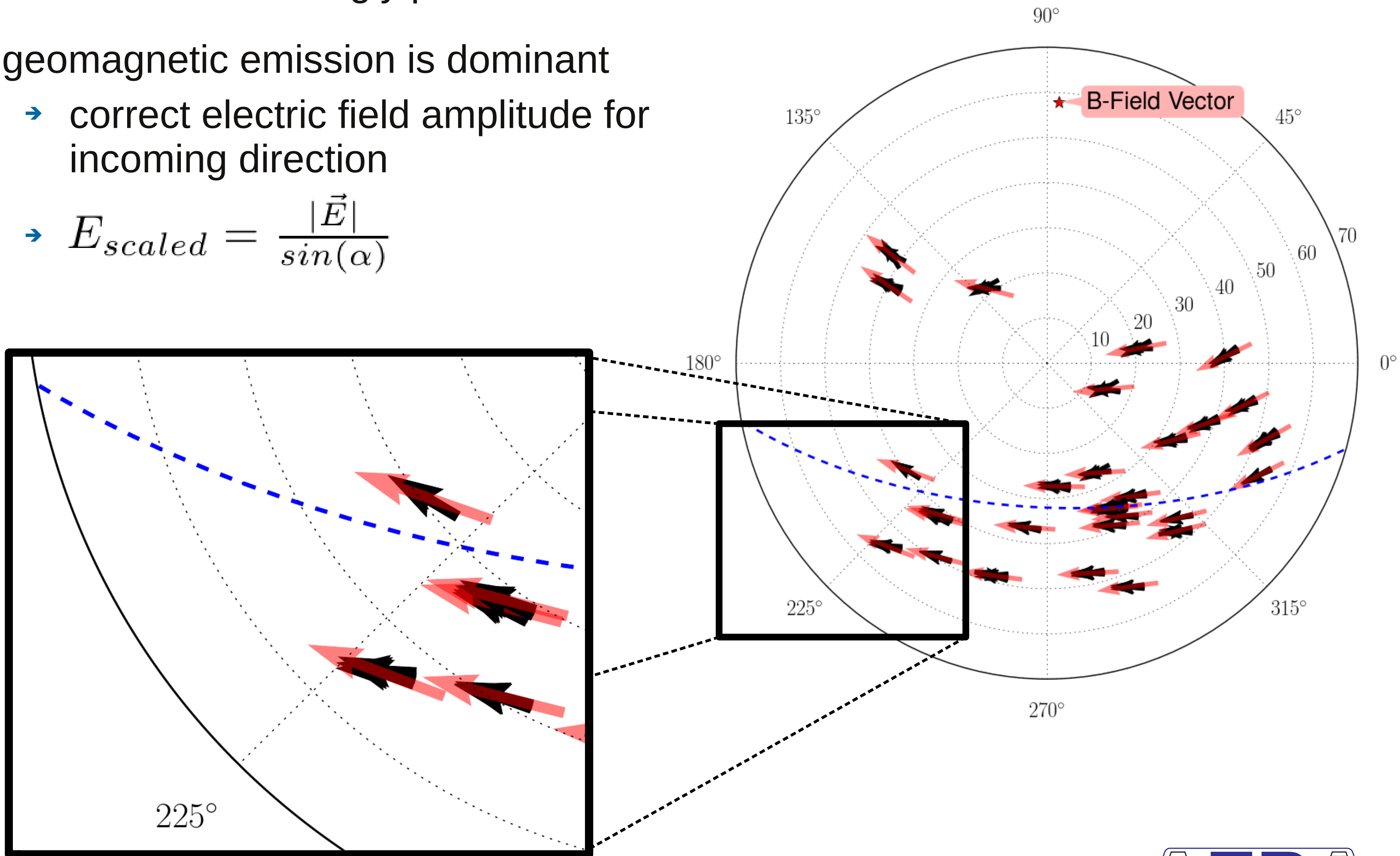

C. Glaser, ARENA (2012)

Auger Engineering Radio Array

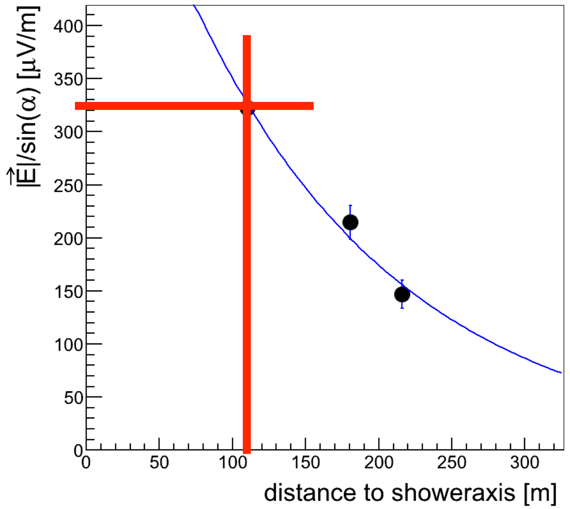

AERA: energy correlation

$$E_{scaled} = \frac{|\vec{E}|}{sin(\alpha)}$$

$$E_{scaled} = A \cdot exp(D/R_0)$$

energy resolution 25%
(incl. surface detector resolution)

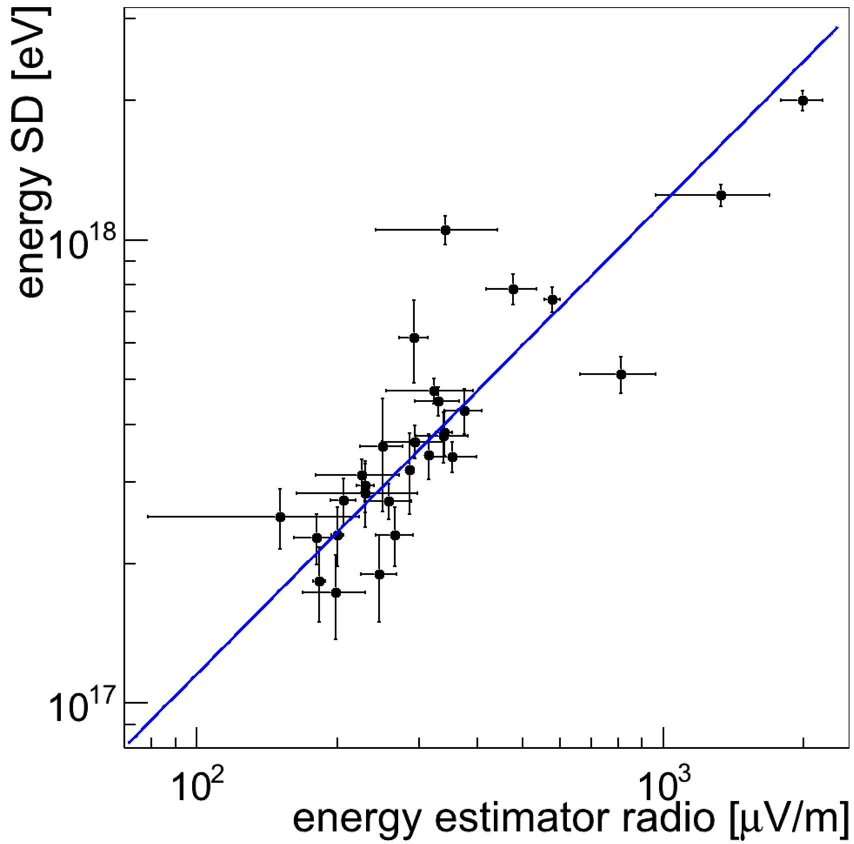

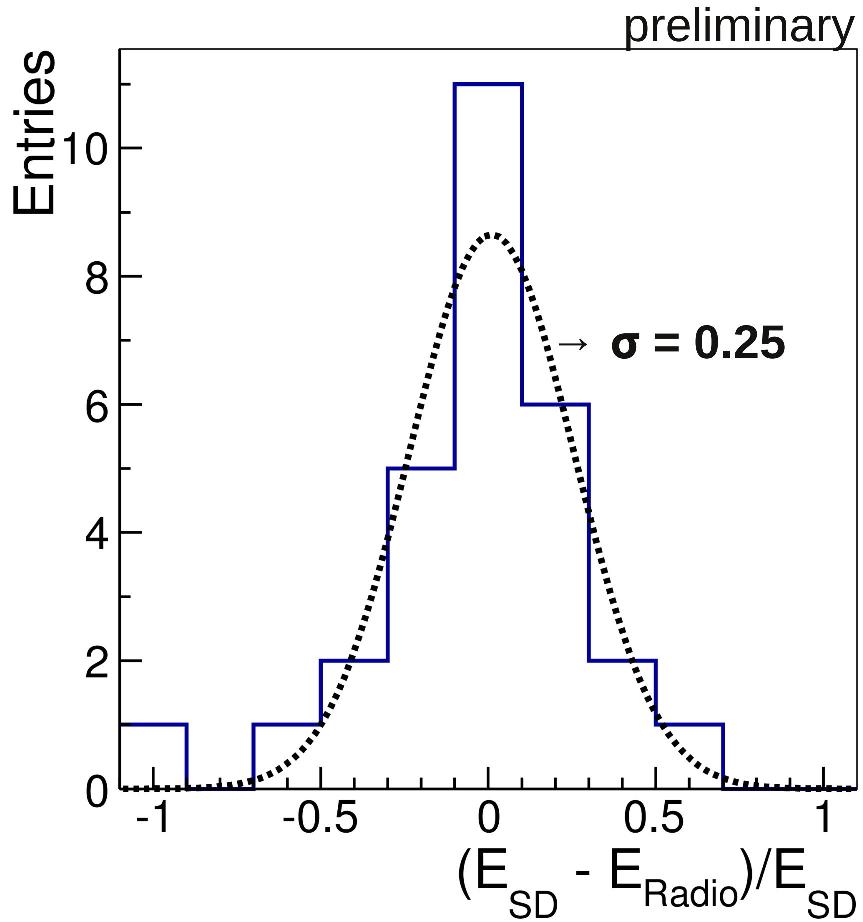

C. Glaser, ARENA (2012)

Energy of air shower

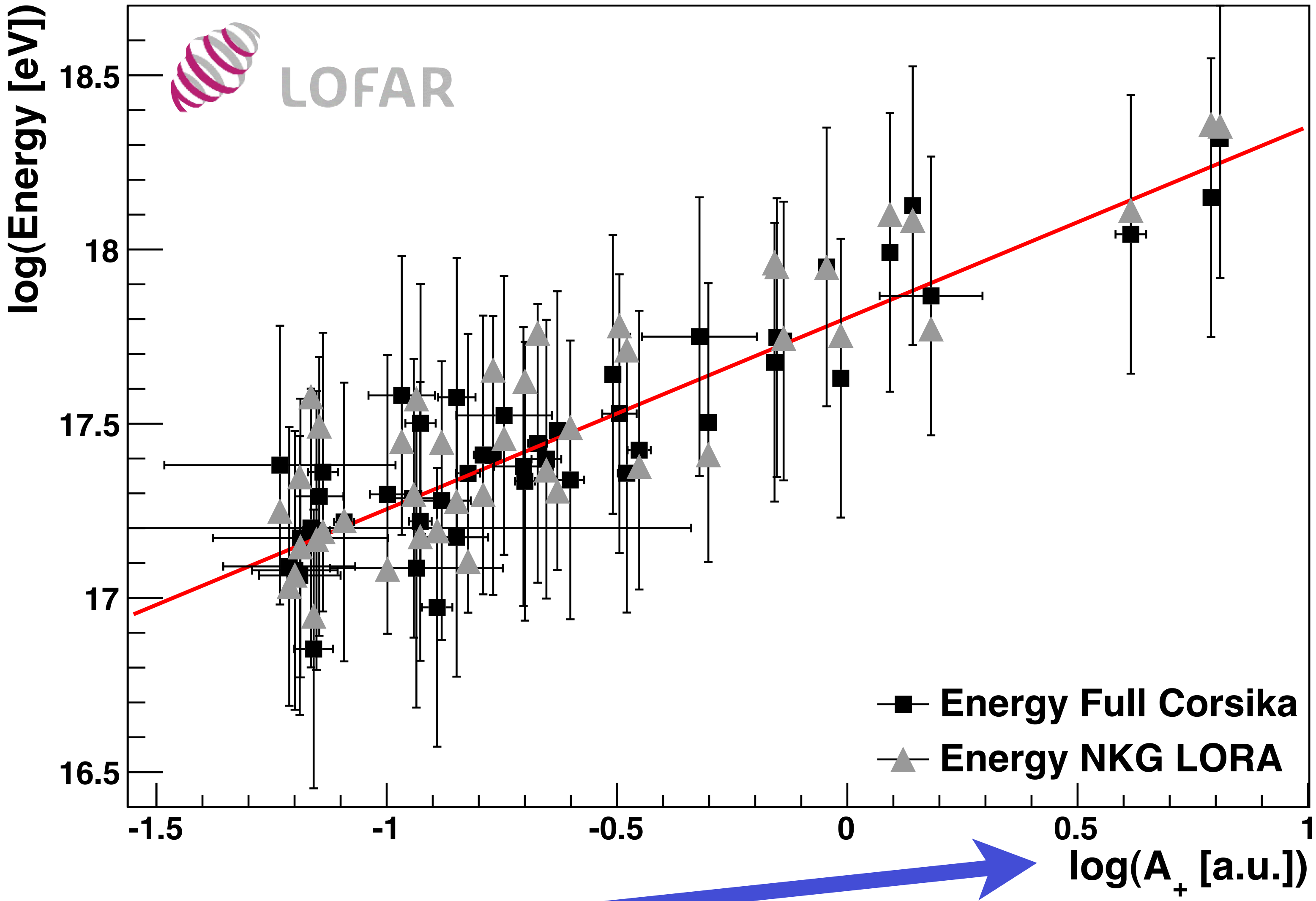

$$P(x',y') = A_+ \cdot \exp\left(\frac{-[(x'-X_+)^2+(y'-Y_+)^2]}{\sigma_+^2}\right) - A_- \cdot \exp\left(\frac{-[(x'-X_-)^2+(y'-Y_-)^2]}{\sigma_-^2}\right) + O$$

Mass (Type)

Depth of the shower maximum Xmax

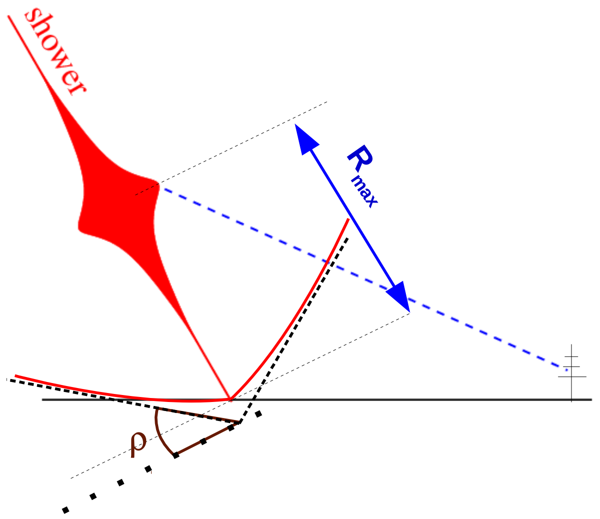

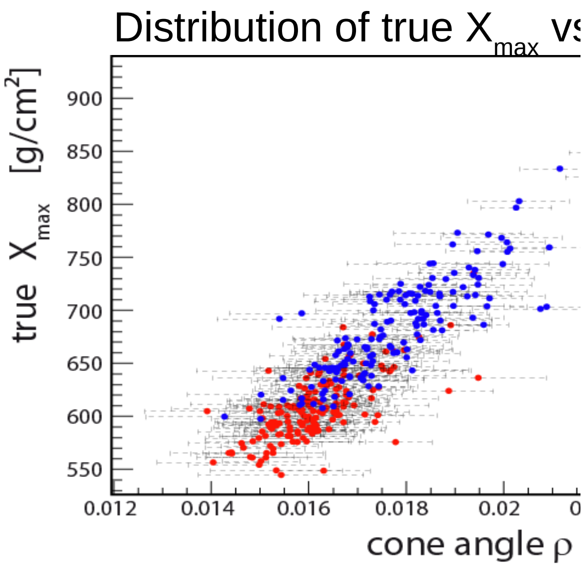

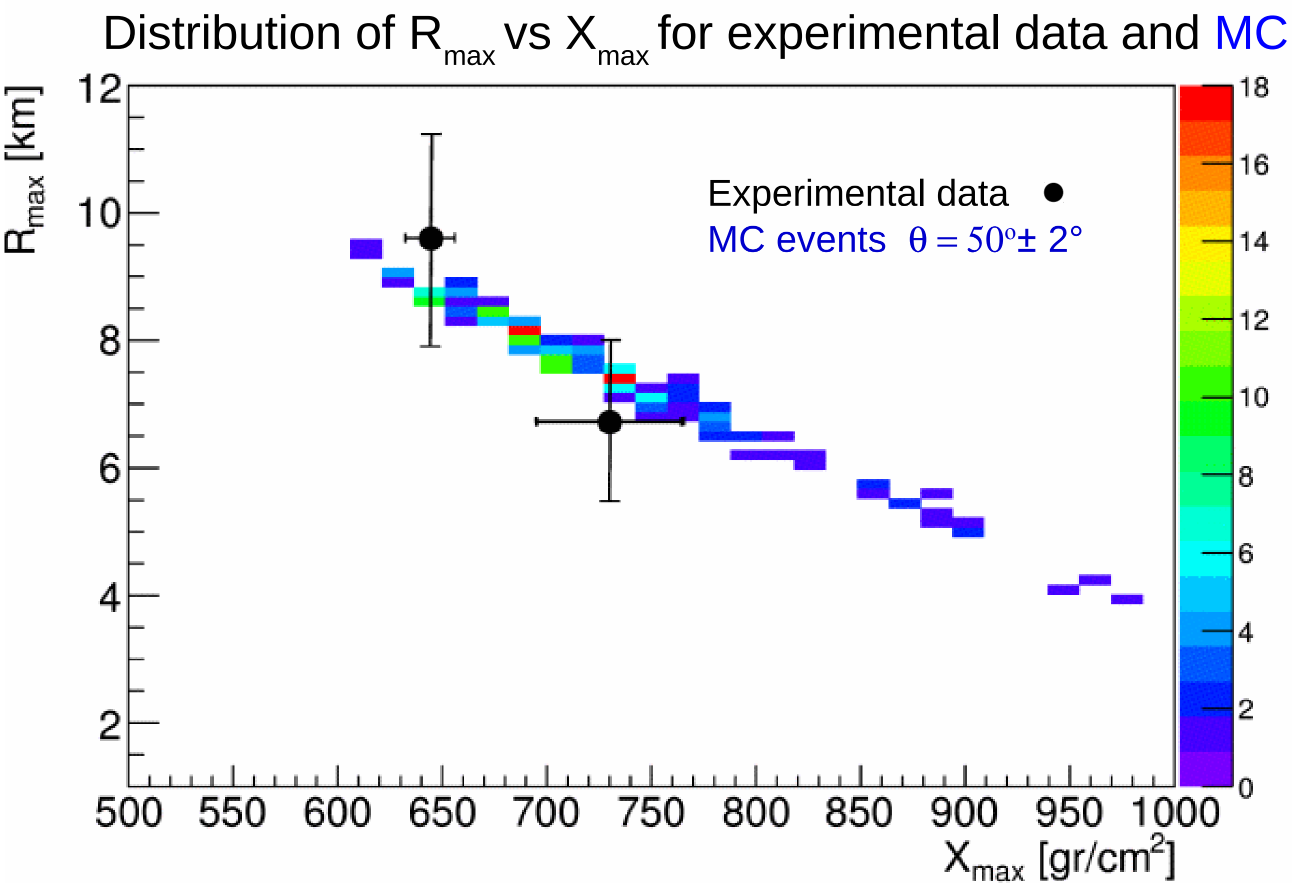

Q. Dorosti (ARENA 2014)

Experimental data: super-hybrid events

Particle type/mass

distance to Xmax

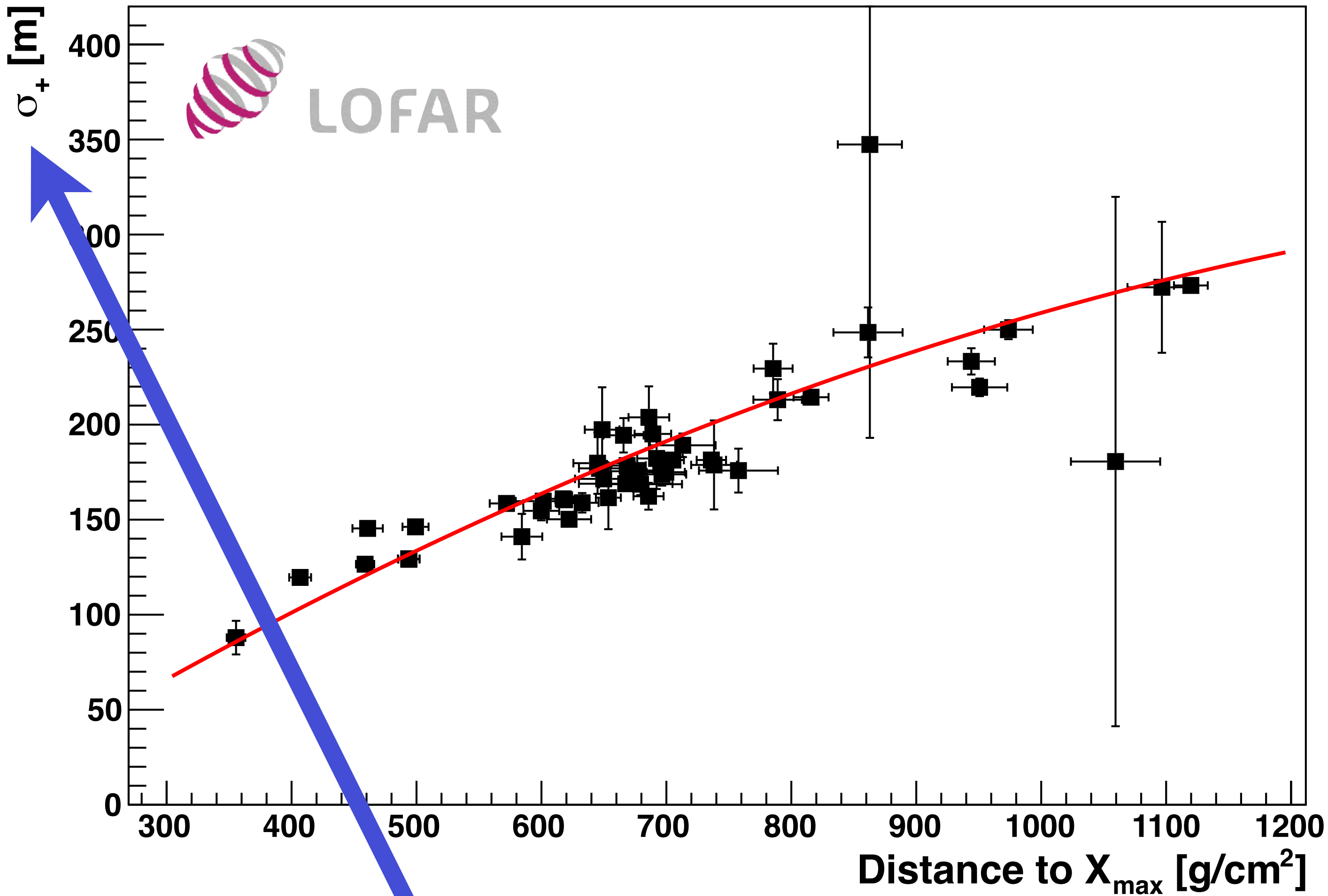

$$P(x', y') = A_+ \cdot \exp\left(\frac{-[(x' - X_+)^2 + (y' - Y_+)^2]}{\sigma_+^2}\right) - A_- \cdot \exp\left(\frac{-[(x' - X_-)^2 + (y' - Y_-)^2]}{\sigma_-^2}\right) + O$$

Reconstruction of the depth of the shower maximum (X_{max})

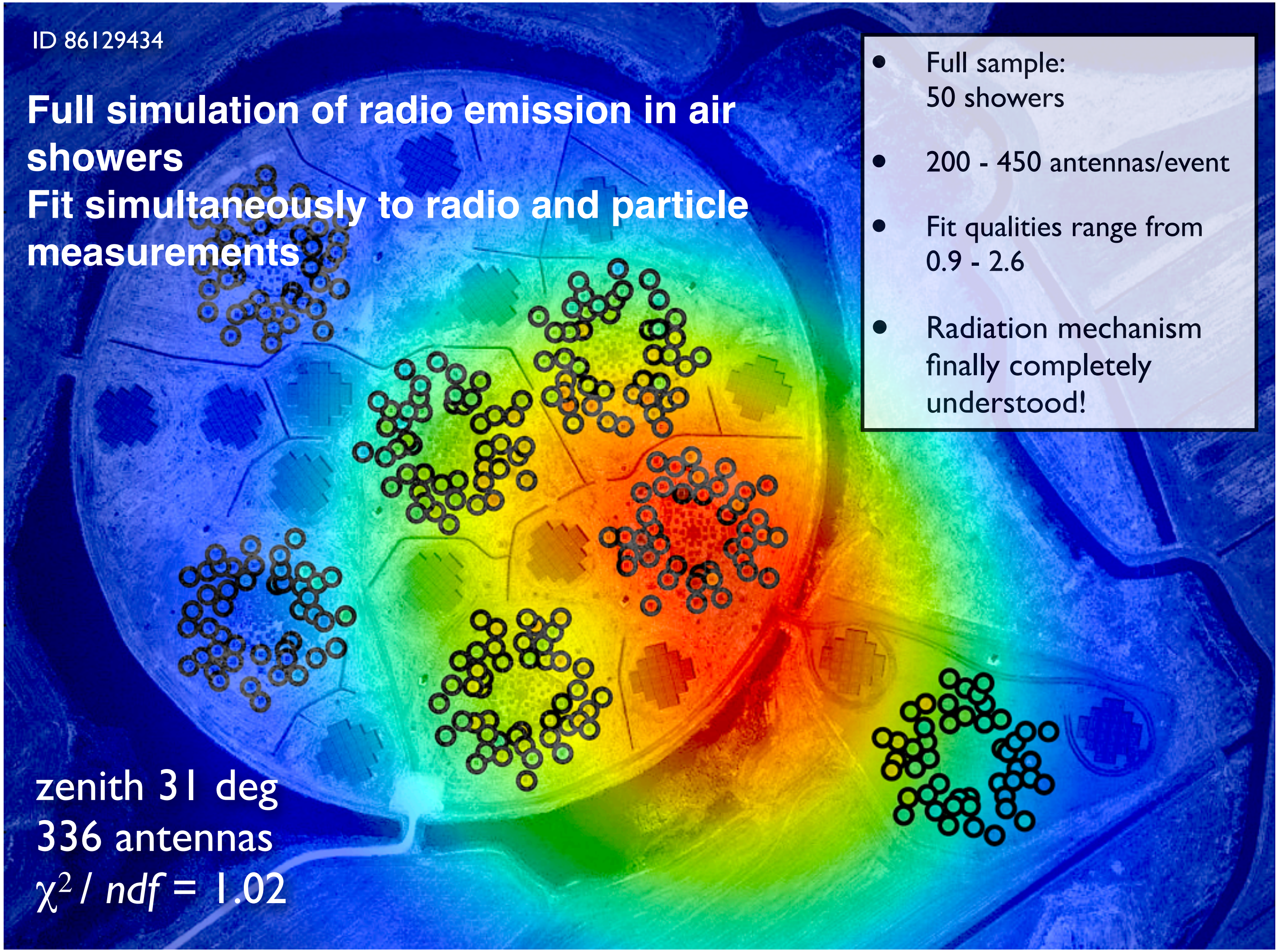

Reconstruction of the depth of the shower maximum (X_{max})

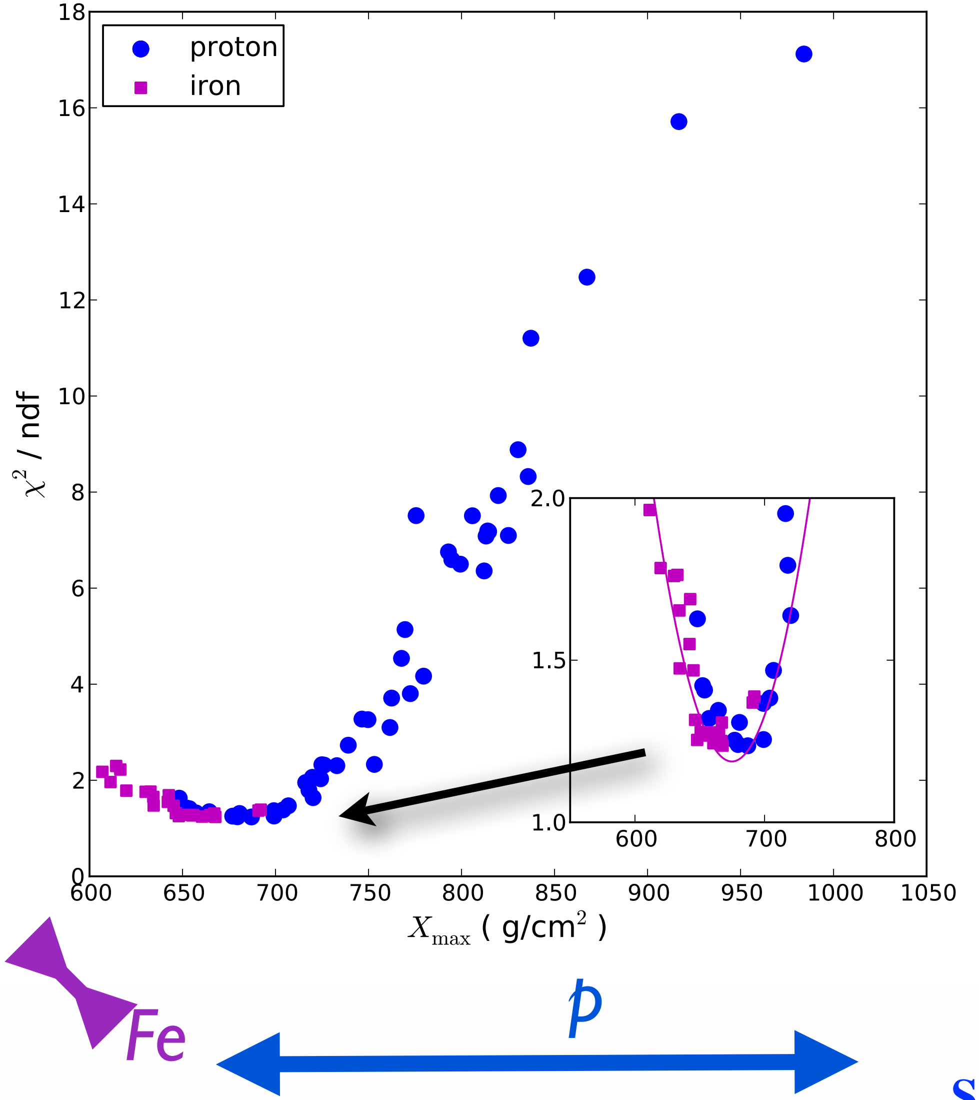

- **For each measured shower:** **Simulate many proton and iron showers**
- **Fit each simulation intensity pattern to the data**
- **Reconstruct depth of shower maximum: Xmax**
- **Uncertainty < 20 g/cm² !!**

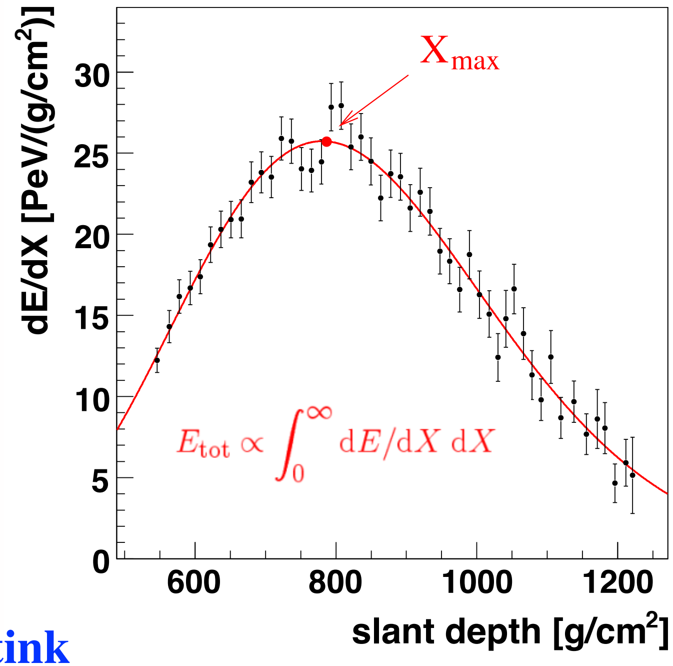

S. Buitink

Precision measurements of radio emission from air showers

- lateral distribution - not rotational symmetric parametrization with two Gaussian functions
- Cherenkov ring in 120 - 240 MHz band
- shape of radio wavefront --> hyperboloid
- polarization --> emission processes (charge excess fraction)
- properties of cosmic rays from radio data
  - direction
  - energy
  - particle type/mass

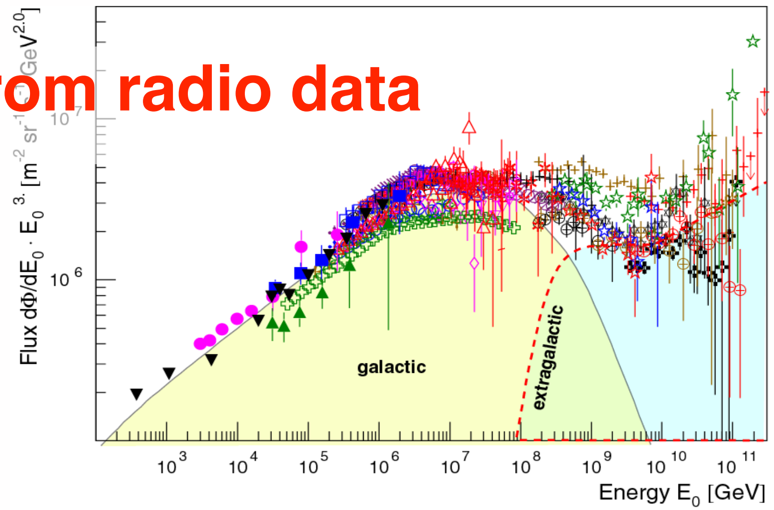

stay tuned, several articles recently accepted and/or submitted

Further reading:

1. LOFAR - The low frequency array, A&A 556 (2013) A2
2. Detecting cosmic rays with the LOFAR radio telescope, A&A 560 (2013) A98
3. LORA: A scintillator array for LOFAR to measure extensive air showers, Nucl. Instr. & Meth. A 767 (2014) 339
4. The all-particle energy spectrum of cosmic rays measured with LORA, in preparation for Astropart. Phys.
5. A parameterization of the radio emission of air showers as predicted by CoREAS simulations and applied to LOFAR measurements, Astropart. Phys. 60 (2015) 13
6. Precision measurement of the shape of the lateral distribution of radio emission in air showers, *almost* submitted to JCAP
7. The shape of the radio wavefront of extensive air showers as measured with LOFAR, Astropart. Phys. 61 (2015) 22
8. Polarized radio emission from extensive air showers measured with LOFAR, JCAP in press, arXiv:1406.1355
9. Measuring a Cherenkov ring in the radio emission from air showers at 110-190 MHz with LOFAR, submitted to Astropart. Phys.
10. A method for high-precision reconstruction of air shower Xmax using two-dimensional radio intensity profiles, PRD in press, arXiv:1408.7001

Further reading:

1. Antennas for the detection of radio emission pulses from cosmic-ray induced air showers at the Pierre Auger Observatory,
   JINST 7 (2012) P10011

2. Advanced functionality for radio analysis in the Offline software framework of the Pierre Auger Observatory,
   Nucl. Instr. & Meth. A 635 (2011) 92

3. Probing the radio emission from air showers with polarization measurements,
   PRD 89 (2014) 052002

4. Energy correlation of the radio signal in air showers, in preparation